THE JOURNAL OF BIOLOGICAL CHEMISTRY VOL. 283, NO. 25, pp. 17635–17651, June 20, 2008
Printed in the U.S.A.

Hyaluronan-CD44 Interaction Activates Stem Cell Marker Nanog, Stat-3-mediated MDR1 Gene Expression, and Ankyrin-regulated Multidrug Efflux in Breast and Ovarian Tumor Cells*

Received for publication, January 7, 2008, and in revised form, April 24, 2008 Published, JBC Papers in Press, April 25, 2008, DOI 10.1074/jbc.M800109200

Lilly Y. W. Bourguignon[1], **Karine Peyrollier, Weiliang Xia, and Eli Gilad**

From the Department of Medicine, University of California, San Francisco, and Endocrine Unit, Veterans Affairs Medical Center, San Francisco, California 94121

Hyaluronan (HA) is a major glycosaminoglycan in the extracellular matrix whose expression is tightly linked to multidrug resistance and tumor progression. In this study we investigated HA-induced interaction between CD44 (a HA receptor) and Nanog (an embryonic stem cell transcription factor) in both human breast tumor cells (MCF-7 cells) and human ovarian tumor cells (SK-OV-3.ipl cells). Using a specific primer pair to amplify Nanog by reverse transcriptase-PCR, we detected the expression of Nanog transcript in both tumor cell lines. In addition, our results reveal that HA binding to these tumor cells promotes Nanog protein association with CD44 followed by Nanog activation and the expression of pluripotent stem cell regulators (*e.g.* Rex1 and Sox2). Nanog also forms a complex with the "signal transducer and activator of transcription protein 3" (Stat-3) in the nucleus leading to Stat-3-specific transcriptional activation and multidrug transporter, *MDR1* (P-glycoprotein) gene expression. Furthermore, we observed that HA-CD44 interaction induces ankyrin (a cytoskeletal protein) binding to MDR1 resulting in the efflux of chemotherapeutic drugs (*e.g.* doxorubicin and paclitaxel (Taxol)) and chemoresistance in these tumor cells. Overexpression of Nanog by transfecting tumor cells with Nanog cDNA stimulates Stat-3 transcriptional activation, MDR1 overexpression, and multidrug resistance. Down regulation of Nanog signaling or ankyrin function (by transfecting tumor cells with Nanog small interfering RNA or ankyrin repeat domain cDNA) not only blocks HA/CD44-mediated tumor cell behaviors but also enhances chemosensitivity. Taken together, these findings suggest that targeting HA/CD44-mediated Nanog-Stat-3 signaling pathways and ankyrin/cytoskeleton function may represent a novel approach to overcome chemotherapy resistance in some breast and ovarian tumor cells displaying stem cell marker properties during tumor progression.

Multidrug resistance frequently contributes to the failure of chemotherapeutic drug treatments in patients diagnosed with solid tumors such as breast and ovarian cancers (1). It is now certain that oncogenic signaling and cytoskeleton function are directly involved in chemotherapeutic drug resistance and tumor progression (2–4). A number of studies have aimed at identifying those molecules that are expressed specifically by epithelial tumor cells and correlate with metastatic behavior and chemoresistance. Among such molecules is hyaluronan (HA),[2] a major component in the extracellular matrix (ECM) of most mammalian tissues (5, 6). HA is a nonsulfated, unbranched glycosaminoglycan consisting of the repeating disaccharide units, D-glucuronic acid and *N*-acetyl-D-glucosamine (5, 6). HA is synthesized by specific HA synthases (6, 7) and digested into various smaller sized molecules by various hyaluronidases (8). It is well known that HA is enriched in many types of tumors (9, 10). In cancer patients, HA concentrations are usually higher in malignant tumors than in corresponding benign or normal tissues. Actually, in some tumor types the level of HA is predictive of malignancy (10). For example, HA levels have been shown to be significantly elevated in the serum of breast cancer patients (11). Also it is believed that tumor cell adhesion to the HA-containing pericellular coat of mesothelial cells is one of the important mechanisms for the peritoneal spread of ovarian cancer (12). HA interacts with a specific cell surface receptor, CD44, which belongs to a family of multifunctional transmembrane glycoproteins expressed in numerous cells and tissues, including breast and ovarian tumor cells and various carcinoma tissues (13–28). CD44 is often expressed in a variety of isoforms that are products of a single gene generated by alternative splicing of variant exons into an extracellular membrane-proximal site (29, 30). In fact, the expression of certain CD44 variant (CD44v) isoforms has been shown to be closely associated with tumor progression (13–28). All CD44 isoforms contain an HA-binding site in their extracellular domain that serves as the major cell surface receptor for HA (31).

Most importantly, HA binding to CD44 stimulates the cytoplasmic domain of CD44 to interact with a number of down-

* This work was supported, in whole or in part, by National Institutes of Health Grants R01 CA66163, R01 CA78633, and P01 AR39448 from the USPHS. This work was also supported by a Veterans Affairs Merit Review grant and a Department of Defense grant. The costs of publication of this article were defrayed in part by the payment of page charges. This article must therefore be hereby marked "*advertisement*" in accordance with 18 U.S.C. Section 1734 solely to indicate this fact.

[1] A Veterans Affairs Research Career Scientist. To whom correspondence and reprint requests should be addressed: Endocrine Unit (111N), Dept. of Medicine, University of California, San Francisco, and Veterans Affairs Medical Center, 4150 Clement St., San Francisco, CA 94121. Tel.: 415-221-4810 (Ext. 3321); Fax: 415-383-1638; E-mail: lilly.bourguignon@ucsf.edu.

[2] The abbreviations used are: HA, hyaluronan; MTT, 3-(4,5-dimethylthiazol-2-yl)-2,5-diphenyltetrazolium bromide; ANOVA, analysis of variance; P-gp, P-glycoprotein; ARD, ankyrin repeat domain; Q-PCR, quantitative PCR; RT, reverse transcriptase; siRNA, small interfering RNA; ECM, extracellular matrix; ES, embryonic stem; SIE, sis-inducible element.

stream effectors, including the cytoskeletal protein, ankyrin (14, 19–21, 32). Ankyrin is a member of membrane skeleton family expressed in a variety of biological systems, including epithelial cells and tissues (33). At the present time, three ankyrin genes have been identified as follows: ankyrin 1 (*Ank1* or ankyrin R), ankyrin 2 (*Ank2* or ankyrin B) and ankyrin 3 (*Ank3* or ankyrin G (34–40), all of which code for ankyrin monomers composed of two highly conserved domains and one variable domain (33). The conserved domains contain a membrane-binding site (~89–95 kDa, also called the ankyrin repeat domain (ARD)) in the N-terminal region (41), and a spectrin-binding domain (≈62 kDa) (42). The striking feature shared by all ankyrin N-terminal domains is a repeating 33-amino acid motif present in 24 contiguous copies (41). The 24 ankyrin repeats within the ARD are known to form binding sites for several distinct membrane protein families, including CD44 (32). Overexpression of ARD in cells transfected with ARDcDNA not only interferes with CD44-ankyrin binding but also impairs HA-dependent and CD44-specific biological activities (43). These observations support the conclusion that CD44-ankyrin interaction is very important for most HA-mediated CD44 functions and tumor cell-specific behaviors (14, 19–21, 32, 43, 44). Therefore, further dissection of the interaction pathways controlling HA/CD44 and ankyrin-mediated signal transduction should aid considerably in understanding the intracellular events underlying breast and ovarian tumor metastasis and progression.

P-glycoprotein (P-gp), the product of the *MDR1 (ABCB1)* gene, is a transmembrane ATP-dependent transporter molecule known to play a critical role in drug fluxes and chemotherapeutic resistance in a variety of cancers (45–48). Interestingly, recent studies indicate that both HA and CD44 are also involved in chemotherapeutic drug resistance in many cancer types (49–55). Specifically, HA binding is capable of stimulating *MDR1* expression and drug resistance in breast tumor cells (52). It is also known that CD44 interacts with P-gp to promote cell migration and the invasion of breast tumor cells (56). In addition, HA/CD44-mediated ErbB2 signaling and PI3 kinase/AKT-related survival pathways have been found to be involved in chemotherapeutic drug resistance in breast tumor cells (52). Recently, we have reported that activation of several other HA-CD44-mediated oncogenic signaling pathways (*e.g.* intracellular Ca^{2+} mobilization (53), epidermal growth factor receptor-mediated extracellular signal-regulated kinase (ERK) signaling (54), and topoisomerase activation (55)) leads to multidrug resistance in head and neck cancer cells. However, the mechanism by which HA/CD44 activates oncogenesis and drug resistance in certain epithelial tumor cells (*e.g.* breast and ovarian cancer cells) has not been fully elucidated.

It has been demonstrated recently that HA is rich in stem cell niches (57). CD44 is expressed in both normal and tumor stem cells (displaying a unique ability to initiate normal and/or tumor cell-specific properties) (58). In fact, CD44 is thought to be one of the important cell surface markers for both normal stem cells and cancer stem cells (58, 59). Furthermore, cancer stem cells have been clearly implicated in the phenomenon of chemoresistance (60, 61). During our search for HA-CD44-induced transcriptional factor(s) that correlate(s) with stem cell functions and possible chemoresistance, we have identified the Nanog family of proteins as a prime candidate. Nanog is an important transcription factor involved in the self-renewal and maintenance of pluripotency in the ICM and of embryonic stem (ES) cells (62, 63). Nanog signaling is regulated by interactions among various pluripotent stem cell regulators (*e.g.* such as Rex1, Sox2, and Oct3/4) which together control the expression of a set of target genes required for ES cell pluripotency (64–66). Constitutive Nanog expression results in the inhibition of ES cell differentiation (63). In response to stress signaling, however, Nanog expression is down-regulated because of DNA damage (67). These findings confirm the essential role of Nanog in regulating a variety of cellular functions. Recently, both breast carcinomas/tumor cells and ovarian dysgerminomas have been shown to express common embryonic stem cell markers, including CD44 and Nanog (13–28, 68, 69). The question of whether there is a direct interaction between CD44 and Nanog in HA-mediated signaling and in breast and ovarian cancer progression has yet to be answered.

Accumulating evidence indicates that the "signal transducer and activator of transcription protein 3" (Stat-3) also plays an important role in regulating cell growth, differentiation, and survival (70, 71). Specifically, activated Stat-3 binds to consensus response elements in the nucleus through its DNA-binding domains, and activates transcription of specific target genes (72, 73). It is known that both the N-terminal region and the coiled-coil domains of Stat-3 are involved in protein-protein interactions that result in activating signaling pathways (70–73). Previous studies have also shown that Nanog functions in parallel with Stat-3 in the maintenance of stem cell properties (74). Thus, it appears that there must be a functional link between Nanog and Stat-3. In addition, abnormal Stat-3 signaling appears to play a critical role in oncogenesis (70–73, 75, 76). Furthermore, Stat-3 overexpression and constitutive activation have been observed in a variety of human malignancies, including breast and ovarian carcinomas (70–73, 77, 78).

The question of whether HA/CD44-mediated signaling influences "cross-talk" between Nanog and Stat-3 during breast and ovarian cancer progression and chemoresistance remains to be answered. In this study we present new evidence that HA stimulates CD44-Nanog complex formation leading to Nanog activation and embryonic stem cell marker expression. HA binding to CD44 also induces Nanog interaction with Stat-3 resulting in Stat-3-specific transcriptional activation, *MDR1* gene expression, and tumor cell growth. Furthermore, we have found that HA-CD44 binding promotes ankyrin association with MDR1 (P-gp) and multidrug fluxes. Consequently, all of these events contribute to HA/CD44-mediated therapeutic drug resistance in both breast and ovarian tumor cells.

MATERIALS AND METHODS

Cell Culture—The human breast tumor cell line MCF-7 cells were purchased from ATCC (Manassas, VA). The SK-OV-3.ipl cell line was established from ascites that developed in a nu/nu mouse given an intraperitoneal injection of SK-OV-3 human ovarian carcinoma cell line (obtained from the American Type

Culture Collection) as described previously (16, 26, 79–81). Both MCF-7 cells and SK-OV-3.ipl cells were grown in RPMI 1640 medium and Dulbecco's modified Eagle's medium/F-12 medium, respectively, supplemented with 10% fetal bovine serum. Cells were routinely serum-starved (and therefore deprived of serum HA) before adding HA.

Antibodies and Reagents—Monoclonal rat anti-CD44 antibody (clone 020; isotype IgG_{2b}; obtained from CMB-TECH, Inc., San Francisco) recognizes a determinant of the HA-binding region common to CD44 and its principal variant isoforms (13–16, 19–28, 79–81). This rat anti-CD44 was routinely used for HA-related blocking experiments and immunoprecipitation. Immunoreagents such as goat anti-Nanog antibody, goat anti-MDR1 (P-glycoprotein 170) antibody, goat anti-actin antibody, and mouse anti-lamin A/C antibody were purchased from Santa Cruz Biotechnology, Inc. (Santa Cruz, CA). Both sheep anti-Rex1 antibody and goat anti-Sox2 antibody were obtained from R & D Systems (Minneapolis, MN). Mouse anti-ankyrin antibody and rabbit anti-Stat-3 antibody were purchased from Millipore (Billerica, MA) and Calbiochem, respectively. [^{14}C]Doxorubicin hydrochloride and [^{3}H]paclitaxel (Taxol) were purchased from Amersham Biosciences and Moravek Biochemicals (Brea, CA), respectively. Nonradioactive doxorubicin hydrochloride and paclitaxel (Taxol) were obtained from Sigma.

Healon HA polymers (~500,000-dalton polymers) purchased from Pharmacia & Upjohn Co. (Kalamazoo, MI) were prepared by gel filtration column chromatography using a Sephacryl S1000 column. The purity of the HA polymers used in our experiments was further verified by anion exchange high performance liquid chromatography followed by protein and endotoxin analyses using BCA protein assay kit (Pierce) and an *in vitro* Limulus amebocyte lysate assay (Cambrex Bio Science Walkersville Inc., Walkersville, MD), respectively. No protein or endotoxin contamination was detected in this HA preparation.

HA fragments digested by PH-20 (bovine testicular hyaluronidase) were prepared according to the method described previously (102, 103). Briefly, healon HA polymers (500 mg) were dissolved in 50 ml of 0.1 M acetate buffer (pH 5.4) containing 0.15 M NaCl and digested with 20,000 units of PH20 (bovine testicular hyaluronidase) (Wyeth Laboratories Inc., Philadelphia) at 37 °C. Ten-milliliter aliquots were removed after 2-, 4-, 6-, 8-, and 24-h intervals, and the reaction was terminated by adding trichloroacetic acid at 10% final concentration (v/v). After standing at 4 °C for at least 4 h, any precipitate was removed by centrifugation at 2,500 × *g* for 30 min. The supernatants were then pooled, dialyzed extensively against distilled water, recentrifuged, and freeze-dried. The HA fragment preparation was dissolved in 10 ml of 0.1 M acetic acid and applied to a column (2.0 × 150 cm) of Sephadex G-50. The column was eluted in 0.1 M acetic acid at the flow of 10 ml/h, and 5-ml fraction were collected. Each fraction was assayed for hyaluronan content, and size ranges of the fragments were determined as described previously (102, 103). The HA fragments (~2–3 disaccharide units) were used in the study.

Preparations of NanogsiRNA and Stat-3 siRNA—The siRNA sequence targeting human Nanog and Stat-3 (from mRNA sequence, GenBank™ accession number NM_024865 and NM_213662, respectively) corresponds to the coding region relative to the first nucleotide of the start codon. Target sequences were selected using the software developed by Ambion. As recommended by Ambion, Nanog- or Stat-3-specific targeted regions were selected beginning 50–100 nucleotides downstream from the start codon. Sequences close to 50% G/C content were chosen. Specifically, Nanog target sequences (target 1, AATCTTCACCTATGCCTGTGA; target 2, AATGAAATCTAAGAGGTGGA; and target 3, AAACCATGGATTTATTCCTAA) and scrambled sequences were used. In the case of Stat-3siRNA, Stat-3-specific target 1, AATCAAGCAGTTTCTTCAGAG, target 2, AATGGAAACAACCAGTCAGTG, target 3, AAATTAAGAAACTGGAGGAGT, and target 4, AAACACTTGACCCTGAGGGAG, and scrambled sequences were used. Both MCF-7 cells and SK-OV-3.ipl cells were then transfected with siRNA using siPORT Lipid as transfection reagent (Silencer™ siRNA transfection kit; Ambion, TX) according to the protocol provided by Ambion. Cells were incubated with 50 pmol of NanogsiRNA or Stat-3siRNA or 50 pmol of siRNA containing scrambled sequences or no siRNA for at least 48 h before biochemical experiments.

Reverse Transcriptase (RT)-PCR—Total RNA was isolated from MCF-7 cells, SK-OV-3.ipl cells, or human skin fibroblasts using Tripure isolation reagent kits (Roche Applied Science). Subsequently, first-stranded cDNAs synthesized from RNA using Superscript first-strand synthesis system was used for RT-PCR in the presence of SUPERSCRIPT II reverse transcriptase (Invitrogen). For the detection of Nanog transcript expression, two Nanog-specific primers (the sense primer 5′-ATGCCTGTGATTTGTGGGCC-3′ and the antisense primer 5′-GCCAGTTGTTTTTCTGCCAC-3′) were designed for this study. For loading controls, two 36B4-specific primers (the sense primer 5′-GCGACCTGGAAGTCCAACTAC-3′ and the antisense primer 5′-ATCTGCTGCATCTGCTTGG-3′) were also used. The reactions were cycled after an initial 5-in denaturation at 94 °C followed by 35 cycles of denaturation at 94 °C for 30 s, annealing at 60 °C for 30 s, and polymerization at 72 °C for 2 min. The PCR products (~403 bp for Nanog; and ~100 bp for 36B4) were then analyzed using a 2.0% agarose gel electrophoresis containing Sybr Safe DNA gel staining. As controls, RT-PCR was carried out in the absence of SUPERSCRIPT II reverse transcriptase or in the absence of template in the PCR mixture. No amplification products were detected in these control samples.

Quantitative PCR (Q-PCR)—Total RNA was isolated from MCF-7 or SK-OV-3.ipl cells (transfected with NanogcDNA or vector alone or treated with NanogsiRNA/Stat-3siRNA or siRNAs with scrambled sequences in the presence or absence of 24 h HA treatment) using Tripure isolation reagent kits (Roche Applied Science) as described above. First-stranded cDNAs were synthesized from RNA using Superscript first-strand synthesis system (Invitrogen). Gene expression was quantified using probe-based Sybr Green PCR master mix kits, ABI PRISM 7900HT sequence detection system, and SDS software (Applied Biosystems, Foster City, CA). A cycle threshold (minimal PCR cycles required for generating a fluorescent signal exceeding a preset threshold) was determined for each gene of

interest and normalized to a cycle threshold for a housekeeping gene (36B4) determined in parallel. The 36B4 is a human acidic ribosomal phosphoprotein P0 whose expression was not changed in tumor cells transfected with plasmid DNAs (*e.g.* NanogcDNA or vector alone) or treated with NanogsiRNA/Stat-3siRNA or siRNAs with scrambled sequences in the presence or absence of 24-h HA treatment. The Q-PCR primers used for detecting gene expression of *MDR1*, *Rex1*, and *Sox2* were as follows. Specifically, two MDR1-specific primers (the sense primer 5′-TGCGACAGGAGATAGGCTG-3′ and the antisense primer 5′-GCCAAAATCACAAGGGTTAGCTT-3′), two Rex1-specific primers (the sense primer 5′-GCGT-CATAAGGGGTGAGTTTT-3′ and the antisense primer 5′-AGAACATTCAAGGGAGCTTGC-3′), and two Sox2-specific primers (the sense primer 5′-GCCGAGTGGAAACTTT-TGTCG-3′ and the antisense primer 5′-GCAGCGTGTACT-TATCCTTCTT-3′) were used. Finally, for detecting 36B4 gene expression, two 36B4-specific primers (the sense primer 5′-GCGACCTGGAAGTCCAACTAC-3′ and the antisense primer 5′-ATCTGCTGCATCTGCTTGG-3′) were used.

Plasmid Construction—The human Nanog expression plasmid was generated by RT-PCR using two Nanog-specific primers (the sense primer 5′-ATGAGTGTGGATCCAGCTTGT-3′ and the antisense primer 5′-TCACGTCTTCAGGTTGCAT-GTT-3′) and SK-OV-3.ipl cDNA as a template. The PCR product was then cloned into pcDNA3.1/CT-GFP-TOPO (Invitrogen) and sequenced. The Stat-3 reporter pGL3SIE was prepared as follows, Stat-3 SIE (TTCTGGGAATTTTCTGG-GAATT) was first synthesized by the Biomolecular Research Center (University of California, San Francisco) and then cloned into pGL3 luciferase reporter vector (Promega) followed by sequence verification. The cDNA encoding the full-length ankyrin repeat domain (ARD) was double-digested with BamHI and EcoRI and ligated in-frame into pcDNA3.1/HisC vector that contains His epitope as described previously (32).

Cell Transfection—To establish a transient expression system, tumor cells (*e.g.* MCF-7 or SK-OV-3.ipl cells) were transfected with plasmid DNAs (*e.g.* NanogcDNA, ARDcDNA, or vector alone) using Lipofectamine 2000 methods (Invitrogen). Briefly, cells were plated at a density of 2×10^6 cells per 100-mm dish and transfected with 25 μg/dish plasmid cDNA using Lipofectamine 2000. Transfected cells were grown in the culture medium for at least 24–48 h. Various transfectants were then analyzed for their protein expression by anti-Nanog and anti-ankyrin-mediated immunoblotting as described below.

Preparations of Cell Lysate, Cytoplasmic, and Nucleus Fractions—Both MCF-7 cells and SK-OV-3.ipl cells (untransfected or transfected with NanogcDNA or vector alone) were serum-starved for 24 h followed by incubation with 50 μg/ml HA (or pretreated with anti-CD44 antibody followed by HA treatment or no HA addition) for various time intervals (*e.g.* 0, 5, or 30 min) at 37 °C. Cells were then lysed in a lysis buffer (50 mM HEPES (pH 7.5), 150 mM NaCl, 20 mM $MgCl_2$, 0.5% Nonidet P-40, 0.2 mM Na_3VO_4, 0.2 mM phenylmethylsulfonyl fluoride, 10 μg/ml leupeptin, and 5 μg/ml aprotinin). Both cytoplasmic and nuclear fractions were prepared using the extraction kit from Active Motif (Carlsbad, CA) according to the protocols provided by the manufacture.

Immunoprecipitation and Immunoblotting Techniques—The cell lysate or the cytosolic fraction isolated from MCF-7 cells or SK-OV-3.ipl cells (untransfected or transfected with NanogcDNA or vector alone in the presence of 50 μg/ml HA or pretreated with anti-CD44 antibody for 1 h followed by HA treatment or no HA addition for various time intervals (*e.g.* 0, 5, or 30 min at 37 °C) was immunoblotted using various immunoreagents (*e.g.* goat anti-Nanog antibody (2 μg/ml), sheep anti-Rex1 antibody (2 μg/ml), goat anti-Sox2 antibody (2 μg/ml), or goat anti-actin antibody (2 μg/ml), respectively).

In addition, immunoprecipitation was conducted after homogenization of the cell lysate using rat anti-CD44 antibody followed by goat anti-rat IgG beads. Subsequently, the immunoprecipitated materials were solubilized in SDS sample buffer, electrophoresed, and blotted onto the nitrocellulose. After blocking nonspecific sites with 3% bovine serum albumin, the nitrocellulose filter was incubated with various antibodies (*e.g.* goat anti-Nanog antibody (2 μg/ml) or rat anti-CD44 antibody (2 μg/ml), respectively) for 1 h at room temperature.

In some cases, the nuclear factions were isolated from MCF-7 cells/SK-OV-3.ipl cells (untransfected or transfected with NanogcDNA or vector alone or treated with NanogsiRNA or scrambled sequence siRNA) that had been incubated with 50 μg/ml HA (or no HA) for various time intervals (*e.g.* 0, 5, or 30 min) at 37 °C. These samples were then processed for immunoblotting using anti-Nanog antibody (2 μg/ml) or anti-lamin A/C (a nucleus-specific marker) antibody (2 μg/ml). In addition, nuclear fractions of both MCF-7 and SK-OV-3.ipl cells were used for goat anti-Nanog antibody-conjugated immunoprecipitation followed by rabbit anti-Stat-3-mediated immunoblot. In some experiments, anti-Nanog-mediated immunoprecipitation followed by rabbit anti-Stat-3 immunoblot of nuclear fractions isolated from MCF-7/SK-OV-3.ipl cells (untransfected or transfected with NanogcDNA or vector alone or treated with NanogsiRNA or scrambled sequence siRNA) was also carried out as described above.

In addition, cell lysates of MCF-7 cells/SK-OV-3.ipl cells (untransfected, transfected with ARDcDNA, or vector alone and incubated with 50 μg/ml HA (or no HA) for various time intervals (*e.g.* 0, 5, or 30 min) at 37 °C) were processed for immunoprecipitation using rat anti-CD44 antibody-conjugated beads followed by immunoblotting with mouse anti-ankyrin antibody and goat anti-MDR1 antibody, respectively.

Luciferase Reporter Assays—MCF7 cells or SK-OV-3.ipl cells (transfected with NanogcDNA or vector alone or NanogsiRNA or siRNA with scrambled sequences) were grown in 6-well plates. After attachment, cells were co-transfected with pGL3SIE (luciferase reporter vector) in the presence or absence of HA (or anti-CD44 antibody plus HA) and a plasmid encoding β-galactosidase to enable normalization for transfection efficiency. After 24 h, expression of the reporter (luciferase) and the control (β-galactosidase) genes was determined using enzyme assays and luminometry as per the manufacturer's (Promega) instructions.

In Vitro Tumor Cell Growth Assays—Both MCF-7 cells and SK-OV-3.ipl cells (untransfected or transfected with

NanogcDNA or ARDcDNA or vector alone or NanogsiRNA, Stat-3siRNA, or siRNA with scrambled sequences, 5×10^3 cells/well) were treated with HA (50 μg/ml) (or pretreated with rat anti-CD44 followed by HA treatment (50 μg/ml) or untreated). These cells were then plated in 96-well culture plates in 0.2 ml of Dulbecco's modified Eagle's medium/F-12 medium supplement (Invitrogen) containing either 0.5% fetal bovine serum or no serum for 24 h at 37 °C in 5% CO_2, 95% air. In each experiment, a total of five plates (6 wells/treatment (*e.g.* HA treatment or rat anti-CD44 plus HA treatment or no treatment)/plate) was used. Experiments were repeated 5–6 times. The *in vitro* growth of these cells was analyzed by measuring increases in cell number using the 3-(4,5-dimethylthiazol-2-yl)-2,5-diphenyltetrazolium bromide (MTT) assays (CellTiter 96® nonradioactive cell proliferation assay according to the procedures provided by Promega) (2). Subsequently, viable cell-mediated reaction products were recorded by a Molecular Devices (Spectra Max 250) enzyme-linked immunosorbent assay reader at a wavelength of 450 nm.

In some experiments, both MCF-7 cells and SK-OV-3.ipl cells (untransfected or transfected with NanogcDNA or ARDcDNA or vector alone or NanogsiRNA, Stat-3siRNA, or siRNA with scrambled sequences; 5×10^3 cells/well) were treated with various concentrations of doxorubicin (4×10^{-9} to 1.75×10^{-5} M) or paclitaxel (3.2×10^{-9} to 1×10^{-5} M) with no HA or with HA (50 μg/ml) or anti-CD44 plus HA or PH20-treated HA. After 24 h of incubation at 37 °C, MTT-based growth assays were analyzed as described above. The percentage of absorbance relative to untreated controls (*i.e.* cells treated with neither HA nor chemotherapeutic drugs) was plotted as a linear function of drug concentration. The 50% inhibitory concentration (IC_{50}) was identified as a concentration of drug required to achieve a 50% growth inhibition relative to untreated controls.

Drug Efflux and Retention Assays—The efflux activities of [^{14}C]doxorubicin hydrochloride or [^{3}H]paclitaxel (Taxol) in tumor cells (*e.g.* MCF-7 cells or SK-OV-3.ipl cells) were conducted according to the procedures described previously (82). Briefly, tumor cells (untransfected or transfected with NanogcDNA or ARDcDNA or vector alone or NanogsiRNA, Stat-3siRNA, or siRNA with scrambled sequences) were grown in 6-well plates (5×10^3 cells/well). One day later, these cells were then switched to Dulbecco's modified Eagle's medium containing either 10 nM [^{14}C]doxorubicin (50 mCi/mmol) or [^{3}H]paclitaxel (3 Ci/mmol). For analyzing the kinetics of drug efflux, tumor cells treated with either [^{14}C]doxorubicin or [^{3}H]paclitaxel for 24 h were washed and incubated in 1 ml of drug-free medium containing HA (50 μg/ml) or no HA or anti-CD44 antibody plus HA. Subsequently, aliquots (100 μl) of medium were removed at various time intervals (0, 20, 40, 60, 90, 120, and 180 min). After the remaining medium was aspirated, cells were washed twice and then harvested. Cell numbers were measured by a hemocytometer and then dissolved in Solvable tissue gel solubilizer. Radioactivity detected in the medium and associated with cells (indicated as intracellular drug retention) was then measured by a liquid scintillation counter.

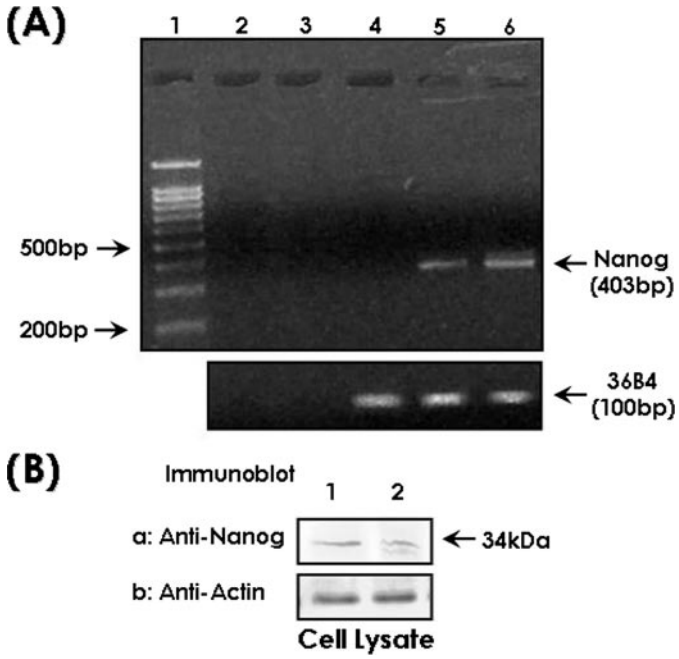

FIGURE 1. **Detection of Nanog expression in tumor cells.** *A,* RT-PCR analysis of Nanog mRNA. Total RNA isolated from various cell types was reverse-transcribed and subjected to PCR using Nanog-specific primer pairs as described under "Materials and Methods." DNA markers (*lane 1*); RT-PCR product of Nanog detected in MCF-7 cells (*lane 2*) or SK-OV-3.ipl cells (*lane 3*) in the absence of reverse transcriptase; RT-PCR product of Nanog detected in normal skin fibroblasts (*lane 4*) or MCF-7 cells (*lane 5*) or SK-OV-3.ipl cells (*lane 6*) in the presence of reverse transcriptase. RT-PCR product of 36B4 detected in samples used in *lanes 4–6* in the presence of reverse transcriptase (as a loading control). *B,* detection of Nanog by anti-Nanog immunoblot analysis. Cell lysates isolated from MCF-7 or SK-OV-3.ipl cells were solubilized by 1% Nonidet P-40 buffer followed by immunoblotting with rabbit anti-Nanog antibody or anti-actin as described under "Materials and Methods." Immunoblot of cell lysates isolated from MCF-7 cells (*lane 1*) or SK-OV-3.ipl cells (*lane 2*) with anti-Nanog antibody (*panel a*) and anti-actin (*panel b*) as a loading control.

RESULTS

Detection of Nanog in Breast Tumor Cells (MCF-7 Cells) and Ovarian Tumor Cells (SK-OV-3.ipl Cells)—Nanog, a recently identified transcription factor, has been shown to play an important role in self-renewal and maintenance of pluripotency in embryonic stem cells (62, 63). Nanog expression has also been detected in a number of tumor cells (68, 69). Using a specific primer pair to amplify the Nanog gene transcript by RT-PCR, we have detected the presence of one PCR product (~403 bp) in both breast tumor cells (MCF-7 cell line) (Fig. 1*A, lane 5*) and ovarian tumor cells (SK-OV-3.ipl cell line) (Fig. 1*A, lane 6*) but not in normal skin fibroblasts (Fig. 1*A, lane 4*). This PCR product was then subcloned into the pcDNA vector from Invitrogen and sequenced. The nucleotide sequence confirms that this band is the Nanog gene transcript. We believe that the RT-PCR is specific because no amplified fragment can be detected in samples incubated without reverse transcriptase (Fig. 1*A, lanes 2* and *3*). The 36B4-specific primers were also used to verify equal sample loading (Fig. 1*A, lanes 4–6*). Our data clearly demonstrate that the Nanog transcript is expressed in both human breast and ovarian tumor cells. Because gene expression at the mRNA level does not always correlate with cellular protein expression, it is important to determine whether Nanog protein expression also occurs in these cells.

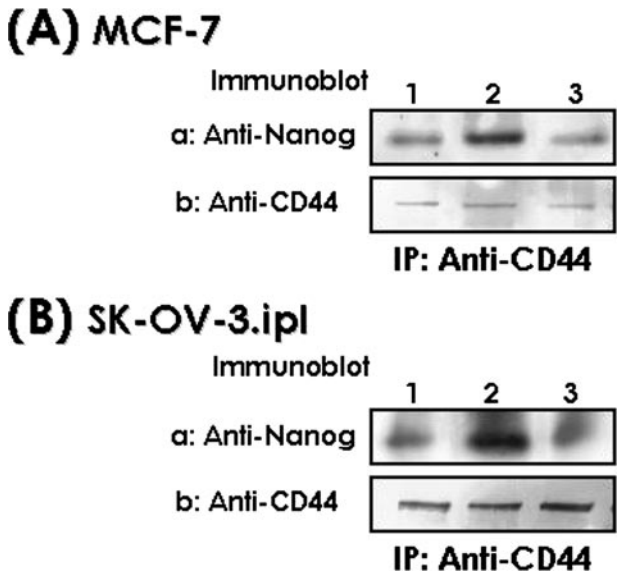

FIGURE 2. **Analysis of HA-mediated CD44-Nanog complex in MCF-7 cells (*A*) and SK-OV-3.ipl cells (*B*).** *A,* cell lysates isolated from MCF-7 cells (untreated (*lane 1*) or treated with HA (50 μg/ml) for 5 min (*lane 2*) or pretreated with anti-CD44 antibody (10 μg/ml) for 1 h followed by 5 min of HA (50 μg/ml) treatment (*lane 3*)) were immunoprecipitated (*IP*) with anti-CD44 antibody followed by immunoblotting with anti-Nanog antibody (*panel a*) or reblotted with anti-CD44 antibody (*panel b*) (as a loading control). *B,* cell lysates isolated from SK-OV-3.ipl cells (untreated (*lane 1*) or treated with HA (50 μg/ml) for 5 min (*lane 2*) or pretreated with anti-CD44 antibody (10 μg/ml) for 1 h followed by 5 min of HA (50 μg/ml) treatment (*lane 3*)) were immunoprecipitated with anti-CD44 antibody followed by immunoblotting with anti-Nanog antibody (*panel a*) or reblotted with anti-CD44 antibody (*panel b*) (as a loading control).

Immunoblot analysis using anti-Nanog antibody indicates that the Nanog gene product (~34-kDa protein) is present in both MCF-7 cells (Fig. 1*B, lane 1*) and SK-OV-3.ipl cells (Fig. 1*B, lane 2*). These results clearly establish that Nanog is expressed at both the transcript and protein levels in MCF-7 cells and SK-OV-3.ipl cells.

HA-mediated CD44 Interaction with Nanog in MCF-7 and SK-OV-3.ipl Cells—A number of studies indicate that HA, CD44, and Nanog are overexpressed in solid tumors, including breast and ovarian cancers, and that these three molecules are all implicated in the initiation and development of malignancy (9–12, 13–28, 68, 69). Thus, identifying the specific extracellular matrix-surface receptor (*i.e.* HA-CD44)-mediated signaling events plus the Nanog function(s) required for activation of epithelial tumor cells could be very important for understanding the disease mechanisms occurring during breast and ovarian tumor progression.

In this study we have first addressed the question of whether there is a physical linkage between CD44 and Nanog in epithelial tumor cells (*e.g.* MCF-7 (Fig. 2*A*) and SK-OV-3.ipl cells (Fig. 2*B*)). To this end we first carried out anti-CD44-mediated immunoprecipitation followed by anti-Nanog immunoblot (Fig. 2, *A, panel a,* and *B, panel a*) or anti-CD44 immunoblot (Fig. 2, *A, panel b,* and *B, panel b*), respectively, using cells treated with HA (or no HA). Our results indicate that a 5-min HA treatment causes the recruitment of a significant amount of Nanog (Fig. 2, *A, panel a, lane 2,* and *B, panel a, lane 2*) into the CD44 complex (Fig. 2, *A, panel b, lane 2,* and *B, panel b, lane 2*). In contrast, a low level of Nanog is present in the anti-CD44-immunoprecipitated materials (reblotted with anti-CD44) in cells treated with no HA (Fig. 2, *A, panels a* and *b, lane 1,* and *B, panels a* and *b, lane 1*) or in cells pretreated with anti-CD44 antibody followed by a 5-min HA treatment (Fig. 2, *A, panels a* and *b, lane 3,* and *B, panels a* and *b, lane 3*). These findings clearly establish that CD44 and Nanog are closely associated with each other, and there is a significant increase in the complex following a 5-min HA treatment of both breast and ovarian tumor cells.

During a 30-min HA treatment of either MCF-7 or SK-OV-3.ipl cells, Nanog expression increases in the nuclear fraction (Fig. 3, *I, panel A*, *a* and *b*, *lane 2,* and *I, panel B, a* and *b, lane 2*). Previous studies showed that activated Nanog functions as a transcription factor that binds to specific promoter elements of target genes and regulates gene expression encoding *Rex1* and *Sox2* (64, 66). In this study we have observed that HA-CD44 binding is capable of stimulating *Rex1* (Fig. 3, *II*, *panel A*, *a, lane 2,* and *II*, *panel B, a, lane 2*) and *Sox2* gene expression (Fig. 3, *II, panel A, b, lane 2,* and *II*, *panel B, b, lane 2*). In contrast, a very low level of Nanog (Fig. 3, *I, panel A, a, lane 1,* and *I, panel B, a, lane 1*) and *Rex1/Sox2* gene expression (Fig. 3, *II, panel A, a, lane 1, II*, *panel A, b, lane 1*, *II, panel B, a, lane 1,* and *II, panel B, b, lane 1*) is detected in both tumor cells treated with no HA. When MCF-7 and SK-OV-3.ipl cells were pretreated with anti-CD44, both HA-mediated Nanog expression (Fig. 3, *I, panel A, a, lane 3,* and *I, panel B, a, lane 3*) and *Rex1/Sox2* gene expression (Fig. 3, *II, panel A, a, lane 3, II, panel A, b, lane 3, II, panel B, a, lane 3,* and *II, panel B, b, lane 3*) are greatly reduced. Therefore, it is likely that Nanog production and certain stem cell regulator gene expression (*e.g. Rex1* and *Sox2*) involves HA-CD44 interaction. Further analyses indicated that HA/CD44-induced stimulation of Nanog (Fig. 3, *I, panel A, a* and *b*, *lane 4,* and *I, panel B, a* and *b, lane 4*) and *Rex1/Sox2* gene expression (Fig. 3, II, *panel A, a, lane 4, II, panel A, b, lane 4, II, panel B, a, lane 4,* and *II, panel B, b, lane 4*) was greatly inhibited in MCF-7 and SK-OV-3.ipl cells transfected with NanogsiRNA, as compared with Nanog production (Fig. 3, *I, panel A, a, lane 5,* and *I, panel B, a, lane 5*) and expression of these stem cell regulator markers (Fig. 3, *II, panel A, a, lane 5, II, panel A, b, lane 5, II, panel B, a, lane 5,* and *II, panel B, b, lane 5*) in tumor cells treated with scrambled sequences. Overexpression of Nanog in both MCF-7 cells and SK-OV-3.ipl cells by transfecting cells with NanogcDNA significantly up-regulates Nanog (Fig. 3, *I, panel A, a, lane 6,* and *I, panel B, a, lane 6*) and *Rex1/Sox2* gene expression (Fig. 3, *II, panel A, a, lane 6, II, panel A, b, lane 6, II, panel B, a, lane 6,* and *II, panel B, b, lane 6*) in these tumor cells. These findings strongly suggest that HA/CD44-mediated Nanog signaling activates Nanog-specific target gene (*e.g. Rex1* and *Sox2*) expression in epithelial tumor cells such as breast (MCF-7 cells) and ovarian tumor cells (SK-OV-3.ipl cells).

HA/CD44-mediated Nanog Interaction with Stat-3 Stimulates Stat-3-specific Transcriptional Activation and Tumor Cell Growth—Constitutive activation of Stat-3, a family of transcription factors, has been detected in both breast carcinomas and ovarian tumors (70–73, 77, 78). Previous studies showed that both Nanog and Stat-3 are functionally coupled during the maintenance of stem cell functions (74). To examine the possible interaction between Nanog and Stat-3 in MCF-7 and

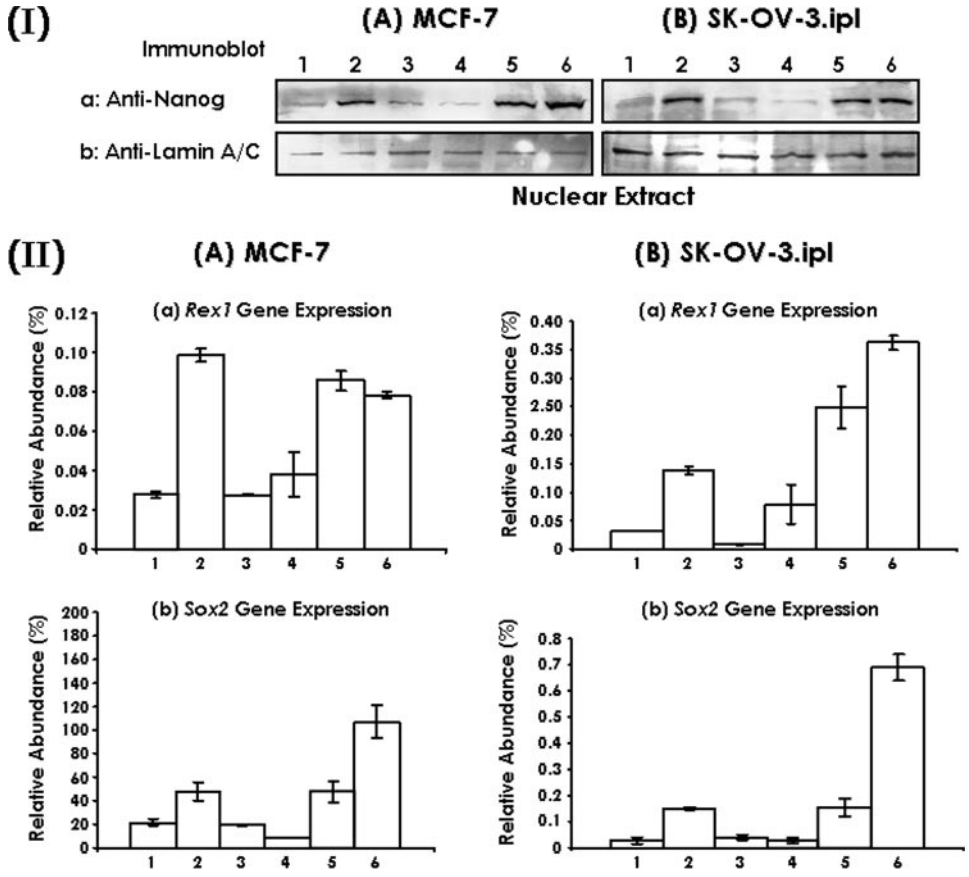

FIGURE 3. **Detection of HA-mediated Nanog nuclear localization in MCF-7 and SK-OV-3.ipl cells.** *I*, nuclear fraction isolated from MCF-7 (*I, panel A*) or SK-OV-3.ipl cells (*I, panel B*) (untreated (*lane 1*) or treated with HA (50 μg/ml) for 30 min (*lane 2*) or pretreated with anti-CD44 for 1 h followed by 30 min of HA (50 μg/ml) treatment (*lane 3*) or pretreated with NanogsiRNA followed by 30 min of HA treatment (*lane 4*) or pretreated with scrambled sequence siRNA followed by 30 min of HA treatment (*lane 5*) or transfected with NanogcDNA (*lane 6*)) were immunoblotted with anti-Nanog antibody (*a*) or anti-lamin A/C antibody (*b*) (as a loading control). *II*, detection of Nanog target gene expression in both MCF-7 (*panel A*) and SK-OV-3.ipl cells (*panel B*). The expression of Nanog target genes (*e.g. Rex1* and *Sox2*) was measured using specific primers and Q-PCR in tumor cells according to the procedures described under "Materials and Methods." Total RNA isolated from either MCF-7 (*panel A*) or SK-OV-3.ipl cells (*panel B*) (untreated (*lane 1*) or treated with HA (50 μg/ml) for 24 h (*lane 2*) or pretreated with anti-CD44 for 1 h followed by 24 h HA (50 μg/ml) treatment (*lane 3*) or pretreated with NanogsiRNA followed by 24 h HA treatment (*lane 4*) or pretreated with scrambled sequence siRNA followed by 24 h HA treatment (*lane 5*) or transfected with NanogcDNA (*lane 6*)) was reverse-transcribed and subjected to Q-PCR using Rex1 (*panel A, a* and *panel B, a*)-specific or Sox2 (*panel A, b* and *panel B, b*)-specific primer pairs as described under "Materials and Methods." Relative mRNA expression levels of Rex1 or Sox2 in various treatments were calculated after normalization with 36B4 mRNA levels as determined by Q-PCR. The values expressed in this figure represent an average of triplicate determinations of three experiments with a standard deviation less than $\pm$5%.

SK-OV-3.ipl cells, we have analyzed the anti-Nanog-mediated immunoprecipitates from nuclear extracts by immunoblotting with anti-Stat-3, or anti-Nanog antibody, respectively. Our results demonstrate that Nanog (Fig. 4, *A, panel b, lane 1,* and *B, panel b, lane 1*) is complexed with Stat-3 (Fig. 4, *A, panel a, lane 1,* and *B, panel a, lane 1*) in the nuclear fractions of both tumor cells without any HA treatment. Furthermore, we have observed that a 30-min HA treatment of MCF-7 or SK-OV-3.ipl cells stimulates a significant increase in the amount of Nanog (Fig. 4, *A, panel b, lane 2,* and *B, panel b, lane 2*) and Stat-3 (Fig. 4, *A, panel a, lane 2,* and *B, panel a, lane 2*) complexes in the nuclear fractions of these tumor cells. When these tumor cells were pretreated with anti-CD44 antibody followed by a 30-min HA treatment, the complex formation between Nanog and Stat-3 in the nuclear fraction is greatly reduced in both cell lines (Fig. 4, *A, panels a* and *b, lane 3,* and *B, panels a* and *b, lane 3*). These findings suggest that Nanog is capable of forming a complex with Stat-3 (in the nucleus) in an HA-dependent and CD44-specific manner.

Stat-3 has also been shown to contain several functional motifs, including a DNA-binding domain, which makes direct contact with Stat-3-binding sites in gene promoters and regulates gene expression (70–73). To determine whether Nanog-associated Stat-3 could lead to transcription activation, we transiently transfected MCF-7 or SK-OV-3.ipl cells with a vector plus a reporter construct, pGL3SIE (containing Stat-3-specific binding sites corresponding to a high affinity mutant of the c-Fos sis-inducible element (SIE) inserted into luciferase reporter vector pGL3), driving expression of firefly luciferase. Our results indicate that the level of transcriptional activation induced by Nanog-associated Stat-3 is low in cells treated with no HA (Fig. 5, *A, lane 1,* and *B, lane 1*) or pretreated with anti-CD44 followed by HA treatment (Fig. 5, *A, lane 3,* and *B, lane 3*). However, transcriptional activation by Nanog-associated Stat-3 is greatly enhanced in both MCF-7 cells and SK-OV-3.ipl cells treated with HA (Fig. 5, *A, lane 2,* and *B, lane 2*). We have also observed that HA-induced Stat-3-specific transcriptional activation was greatly reduced in MCF-7 and SK-OV-3.ipl cells transfected with NanogsiRNA (Fig. 5, *A, lane 4,* and *B, lane 4*), as compared with HA-mediated transcriptional activities detected in tumor cells treated with siRNA with scrambled sequences (Fig. 5, *A, lane 5,* and *B, lane 5*). Overexpression of Nanog by transfecting MCF-7 and SK-OV-3.ipl cells with NanogcDNA greatly enhances Stat-3-mediated transcriptional activation (Fig. 5, *A, lane 6,* and *B, lane 6*). These findings clearly indicate that HA/CD44-activated Nanog plays an important role in regulating Stat-3-specific transcriptional activation in both breast and ovarian tumor cells. There is substantial evidence of Stat-3 involvement in regulating tumor cell survival and growth through the expression of Stat-3 target genes encoding proliferation-related proteins, such as cyclin D1 and c-*Myc* (72, 73, 83). In this study we have observed that both MCF-7 and SK-OV-3.ipl cells undergo rapid cell growth during HA treatment (Tables 1–3). However, pretreatment of these tumor cells with anti-CD44 antibody causes a significant inhi-

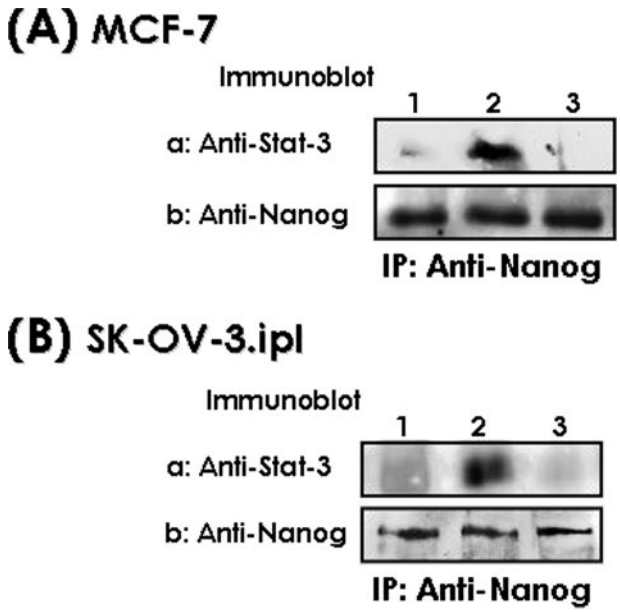

FIGURE 4. **Analysis of HA-mediated Nanog-Stat-3 complex formation in the nuclear fraction of MCF-7 cells (*A*) and SK-OV-3.ipl cells (*B*).** *A,* nuclear fraction isolated from MCF-7 cells (untreated (*lane 1*) or treated with HA (50 μg/ml) for 30 min (*lane 2*) or pretreated with anti-CD44 antibody (10 μg/ml) for 1 h followed by 30 min of HA (50 μg/ml) incubation (*lane 3*)) were immunoprecipitated (*IP*) with anti-Nanog antibody followed by immunoblotting with anti-Stat-3 antibody (*panel a*) or reblotted with anti-Nanog antibody (*panel b*) (as a loading control). *B,* nuclear fraction isolated from SK-OV-3.ipl cells (untreated (*lane 1*) or treated with HA (50 μg/ml) for 30 min (*lane 2*) or pretreated with anti-CD44 antibody (10 μg/ml) for 1 h followed by 30 min HA (50 μg/ml) incubation (*lane 3*)) were immunoprecipitated with anti-Nanog antibody followed by immunoblotting with anti-Stat-3 antibody (*panel a*) or reblotted with anti-Nanog antibody (*panel b*) (as a loading control).

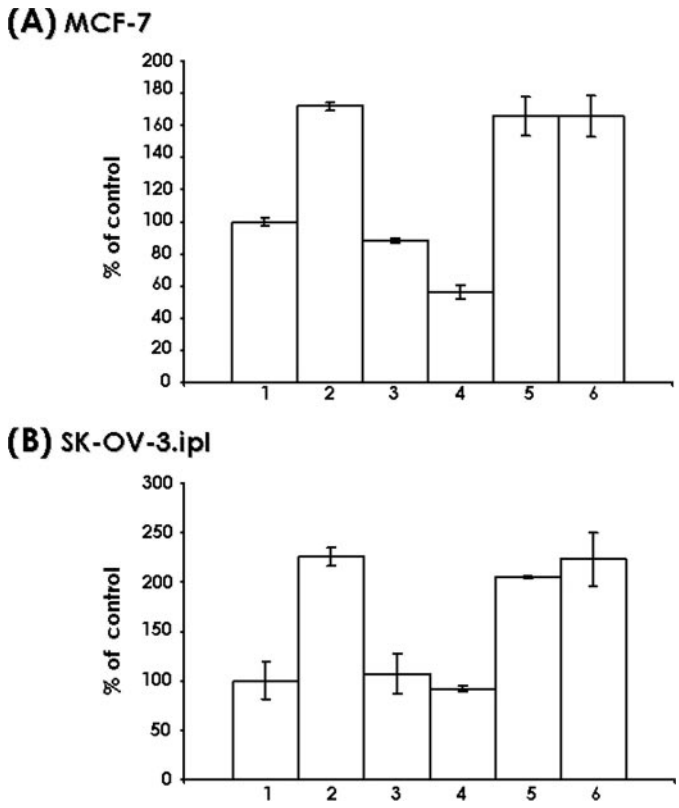

FIGURE 5. **Detection of Stat-3-specific transcriptional activity in tumor cells.** Specifically, MCF-7 cells (*A*) or SK-OV-3.ipl cells (*B*) (untreated (*lane 1*) or treated with HA (50 μg/ml) for 24 h (*lane 2*) or pretreated with anti-CD44 for 1 h followed by 24 h of HA (50 μg/ml) treatment (*lane 3*) or pretreated with NanogsiRNA followed by 24 h of HA treatment (*lane 4*) or pretreated with scrambled sequence siRNA followed by 24 h of HA treatment (*lane 5*) or transfected with NanogcDNA (*lane 6*)) were co-transfected with pGL3SIE (luciferase reporter vector) in the presence or absence of HA (or anti-CD44 antibody plus HA) and a plasmid encoding β-galactosidase (to enable normalization for transfection efficiency). After 24 h, expression of the reporter (luciferase) and the control (β-galactosidase) genes were determined using enzyme assays and luminometry as described under "Materials and Methods." The values expressed in this figure represent an average of triplicate determinations of 3–5 experiments with an S.D. of less than $\pm$5%.

bition of HA-mediated tumor cell growth (Table 1*A*). Overexpression of Nanog by transfecting cells with NanogcDNA upregulates tumor cell growth (Table 2). Importantly, transfection of MCF-7 cells or SK-OV-3.ipl cells with NanogsiRNA or Stat-3siRNA (but not scrambled sequence siRNA) also effectively blocks tumor cell growth (Table 1*B* and Table 3). Together these findings support the conclusion that both Nanog function and Stat-3 activation act as important signaling regulators of HA/CD44-mediated tumor cell growth.

HA/CD44 and Nanog/Stat-3-mediated MDR1 Gene Expression and Multidrug Resistance in MCF-7 and SK-OV-3.ipl Cells—The multidrug-resistant phenotype constitutes a major clinical problem in human cancers, including breast and ovarian cancers (1). Up-regulation of certain membrane pumps, such as MDR1 (P-gp), is known to be involved in the drug efflux and multidrug resistance of solid tumors (45–48). A number of studies have indicated that HA-CD44 interaction induces transcriptional up-regulation of the *MDR1* gene and the expression of multidrug resistance in different cell types (49–55). However, the cellular and molecular mechanisms underlying regulation of *MDR1* gene expression are not well understood. To investigate whether HA/CD44 activation of Nanog-Stat-3 signaling pathway participates in *MDR1* gene expression, we have used *MDR-1*-specific primers and Q-PCR to measure the level of *MDR1* gene expression in both MCF-7 cells and SK-OV-3 cells. Our data indicate that the level of *MDR1* gene expression is significantly enhanced in both MCF-7 cells (Fig. 6*A, lane 2*) and SK-OV-3.ipl cells (Fig. 6*B, lane 2*) treated with HA. In contrast, *MDR1* gene expression is relatively low in either MCF-7 cells (Fig. 6*A, lane 1*) or SK-OV-3.ipl cells (Fig. 6*B, lane 1*) without any HA treatment or those cells pretreated with anti-CD44 antibody followed by HA treatment (Fig. 6, *A, lane 3,* and *B, lane 3*). These observations clearly indicate that HA-mediated *MDR1* gene expression is CD44-dependent. Most importantly, Nanog overexpression caused by transfecting the tumor cells with NanogcDNA significantly upregulates *MDR1* mRNA expression (Fig. 6, *A, lane 4.* and *B, lane 4*). Down-regulation of Nanog or Stat-3 by treating cells with NanogsiRNA (Fig. 6, *A, lane 5,* and *B, lane 5*) or Stat-3siRNA (Fig. 6, *A, lane 6,* and *B, lane 6*), respectively, significantly inhibits HA/CD44-activated *MDR1* mRNA expression. These findings support the conclusion that the Nanog/Stat-3 signaling pathway plays an important part in HA/CD44-mediated *MDR1* gene expression in both breast and ovarian tumor cells.

To further investigate whether multidrug resistance in both MCF-7 cells and SK-OV-3.ipl cells might be through HA-CD44 interaction with Nanog and Stat-3 signaling events, we performed tumor cell growth assays with anti-breast cancer and anti-ovarian cancer chemotherapeutic drugs (*e.g.* doxorubicin

TABLE 1

Analyses of HA-mediated tumor cell growth

Procedures for measuring tumor cell growth in MCF-7 and SK-OV-3.ipl cells (untreated or treated with 50 pmol of NanogsiRNA, or 50 pmol of siRNA-scrambled sequence or 10 μg/ml anti-CD44 antibody) in the presence or absence of 50 μg/ml HA for 24 h were described under "Materials and Methods." Tumor cell growth without any treatment (A) or treated with NanogsiRNA-scrambled sequences (B) is designated as 100%. For the tumor cell growth assay, data represent mean ± S.E. of cell numbers in each sample.

Cells	MCF-7 cell growth		SK-OV-3.ipl cell growth	
	−HA	+HA	−HA	+HA
	% control[a]		*% control*[b]	
A. Effects of anti-CD44 antibody treatment on HA-mediated tumor cell growth				
Untreated cells (control)	100 ± 4	243 ± 6[a]	100 ± 3	255 ± 6[b]
Normal rat IgG-treated cells	97 ± 3[a]	240 ± 5[a]	96 ± 2[b]	258 ± 7[b]
Rat anti-CD44-treated cells	86 ± 2[a]	98 ± 3[a]	91 ± 2[b]	97 ± 3
B. Effects of NanogsiRNA treatment on HA-mediated tumor cell growth				
Scrambled sequence treatment (control)	100 ± 4	247 ± 6[c]	100 ± 4	250 ± 7[d]
NanogsiRNA treatment	78 ± 2[c]	83 ± 4[c]	84 ± 3[d]	92 ± 3[d]

[a] Data are significantly different ($p < 0.005$; ANOVA; $n = 5$) as compared with control samples (*e.g.* untreated (no antibody treatment and no HA addition) (control) samples).
[b] Data are significantly different ($p < 0.001$; ANOVA; $n = 6$) as compared with control samples (*e.g.* untreated (no antibody treatment and no HA addition) (control) samples).
[c] Data are significantly different ($p < 0.005$; ANOVA; $n = 5$) as compared with control samples (*e.g.* scrambled sequence treated (in the absence of HA) (control) samples).
[d] Data are significantly different ($p < 0.005$; ANOVA; $n = 6$) as compared with control samples (*e.g.* scrambled sequence treated (in the absence of HA) (control) samples).

TABLE 2

Effects of Nanog overexpression on HA-mediated tumor cell growth

Procedures for measuring tumor cell growth in MCF-7 and SK-OV-3.ipl cells (transfected with NanogcDNA or vector alone) in the presence or absence of 50 μg/ml HA for 24 h were described under "Materials and Methods." Tumor cell growth or transfected with vector is designated as 100%. For the tumor cell growth assay, data represent mean ± S.E. of cell numbers in each sample.

Cells	Tumor cell growth	
	MCF-7 cells	SK-OV-3.ipl cells
	% of control[a,b]	
Vector-transfected cells (control)	100 ± 3	100 ± 4
NanogcDNA-transfected cells	258 ± 7[a]	265 ± 8[b]

[a] Data are significantly different ($p < 0.001$; ANOVA; $n = 5$) as compared with control samples (*e.g.* vector-transfected (control) samples).
[b] Data are significantly different ($p < 0.001$; ANOVA; $n = 6$) as compared with control samples (*e.g.* vector-transfected (control) samples).

TABLE 3

Effects of Stat-3siRNA treatment on HA-mediated tumor cell growth

Procedures for measuring tumor cell growth in MCF-7 and SK-OV-3.ipl cells (treated with 50 pmol of Stat-3siRNA, or 50 pmol of siRNA-scrambled sequence) in the presence or absence of 50 μg/ml HA for 24 h were described under "Materials and Methods." Tumor cell growth treated with Stat-3siRNA-scrambled sequences is designated as 100%. For the tumor cell growth assay, data represent mean ± S.E. of cell numbers in each sample.

Cells	MCF-7 cell growth		SK-OV-3.ipl cell growth	
	−HA	+HA	−HA	+HA
	% of control[a]		*% of control*[b]	
Scrambled sequence treatment (control)	100 ± 2	253 ± 6[a]	100 ± 3	264 ± 7[b]
Stat-3siRNA treatment	88 ± 3[a]	92 ± 4[a]	95 ± 2[b]	102 ± 2[b]

[a] Data are significantly different ($p < 0.005$; ANOVA; $n = 6$) as compared with control samples (*e.g.* scrambled sequence treated (in the absence of HA) (control) samples).
[b] Data are significantly different ($p < 0.001$; ANOVA; $n = 5$) as compared with control samples (*e.g.* scrambled sequence treated (in the absence of HA) (control) samples).

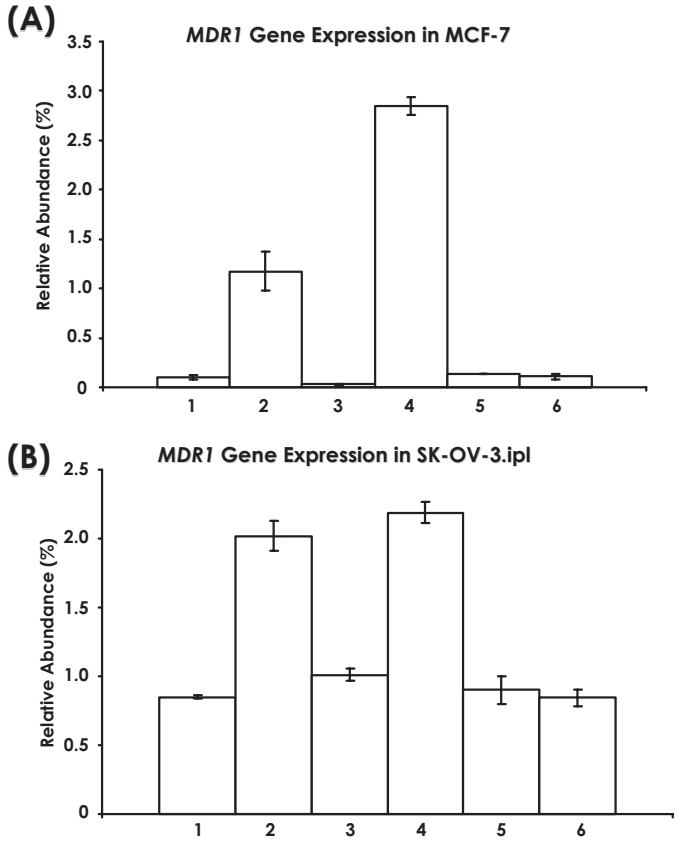

FIGURE 6. **Detection of *MDR1* gene expression in both MCF-7 (*A*) and SK-OV-3.ipl cells (*B*).** The expression of *MDR1* was measured using specific primers and Q-PCR in tumor cells according to the procedures described under "Materials and Methods." Total RNA isolated from either MCF-7 (*A*) or SK-OV-3.ipl cells (*B*) (untreated (*lane 1*) or treated with HA (50 μg/ml) for 24 h (*lane 2*) or pretreated with anti-CD44 for 1 h followed by 24 h of HA (50 μg/ml) treatment (*lane 3*) or transfected with NanogcDNA (*lane 4*) or pretreated with NanogsiRNA followed by 24 h of HA treatment (*lane 5*) or pretreated with Stat-3siRNA followed by 24 h of HA treatment (*lane 6*)) was reverse-transcribed and subjected to Q-PCR using MDR1-specific primer pairs as described under "Materials and Methods." Relative mRNA expression levels of MDR1 in various treatments were calculated after normalization with 36B4 mRNA levels as determined by Q-PCR. The values expressed in this figure represent an average of triplicate determinations of three experiments with an S.D. of less than ±5%.

and paclitaxel in the presence or absence of HA or anti-CD44 antibody plus HA). In the absence of HA, doxorubicin-treated MCF-7 and SK-OV-3.ipl tumor cell growth displays IC_{50} values of 63 and 354 nM, respectively, whereas paclitaxel-treated MCF-7 and SK-OV-3.ipl tumor cell growth exhibits IC_{50} values of 40 and 158 nM, respectively (Fig. 7*I, panel A,* and *II, panel A,* and Tables 4 and 5). However, the binding of HA reduces the ability of both doxorubicin (with IC_{50} values of 316 and 1995 nM, respectively, for MCF-7 and SK-OV-3.ipl cells) and paclitaxel (with IC_{50} values of 158 and 1000 nM, respectively, for MCF-7 cells and SK-OV-3.ipl cells) to cause tumor cell death (Fig. 7, *I, panel A,* and *II, panel A,* and Tables 4 and 5). These observations suggest that HA causes these tumor cells to become relatively resistant to doxorubicin and paclitaxel. Furthermore, pretreatment of these tumor cells with anti-CD44 antibody followed by HA addition greatly reduces the HA-mediated drug resistance (Fig. 7, *I, panel A,* and *II, panel A,* and Tables 4 and 5). This suggests that HA acts through CD44 to support cell survival in the presence of chemotherapeutic drugs

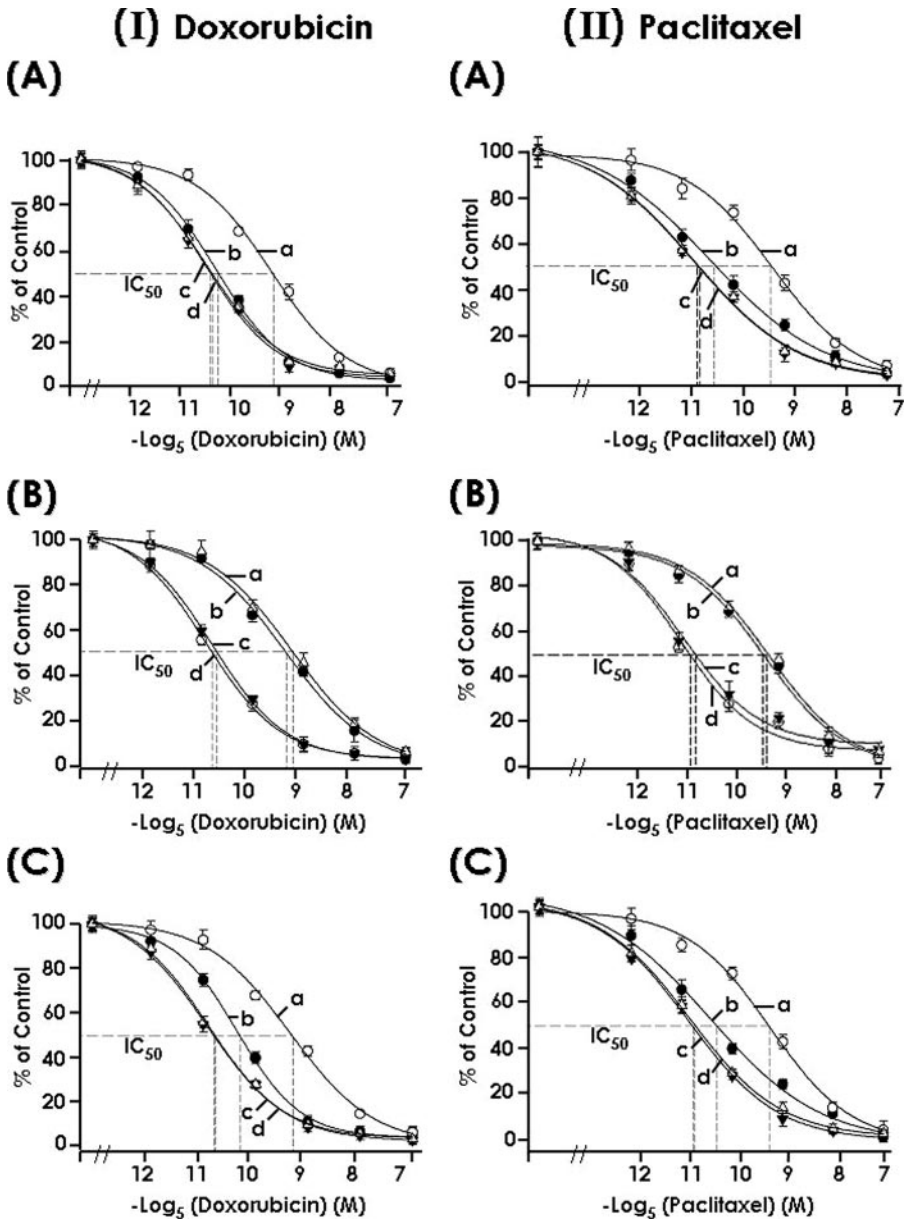

FIGURE 7. **IC_{50} analyses of doxorubicin (*I*) and paclitaxel (*II*) in MCF-7 cells.** MCF-7 cells (untransfected or transfected with NanogcDNA or ARDcDNA or vector alone or NanogsiRNA, Stat-3siRNA, or siRNA with scrambled sequences) (5×10^3 cells/well) were treated with various concentrations of doxorubicin (4×10^{-9} to 1.75×10^{-5} M) (*panel A*) or paclitaxel (3.2×10^{-9} to 1×10^{-5} M) (*panel B*) with no HA or with HA (50 μg/ml) or anti-CD44 plus HA. After 24 h of incubation at 37 °C, MTT-based growth assays were analyzed as described under "Materials and Methods." The percentage of absorbance relative to untreated controls (cells treated with neither HA nor chemotherapeutic drugs) was plotted as a linear function of drug concentration. The 50% inhibitory concentration (IC_{50}) was identified as a concentration of drug required to achieve a 50% growth inhibition relative to untreated controls. *I, panel A, a–d,* MCF-7 cells (untreated (*b*) or treated with HA (50 μg/ml) for 24 h (*a*) or pretreated with anti-CD44 for 1 h followed by no HA treatment (*c*) or with 24 h of HA treatment (*d*)) were incubated with various concentrations of doxorubicin (4×10^{-9} to 1.75×10^{-5} M). *I, panel B, a–d,* MCF-7 cells (transfected with NanogcDNA (*a*) or treated with scrambled sequence siRNA plus 24 h of HA (50 μg/ml) treatment (*b*) or treated with NanogsiRNA plus 24 h of HA treatment (*c*) or Stat-3siRNA plus 24 h of HA treatment (*d*)) were incubated with various concentrations of doxorubicin (4×10^{-9} to 1.75×10^{-5} M). *I, panel C, a–d,* MCF-7 cells (transfected with vector alone plus 24 h of HA (50 μg/ml) treatment (*a*) or no HA (*b*) or transfected with ARDcDNA with no HA (*c*) or with 24 h of HA treatment (*d*)) were incubated with various concentrations of doxorubicin (4×10^{-9} to 1.75×10^{-5} M). *II, panel A, a–d,* MCF-7 cells (untreated (*b*) or treated with HA (50 μg/ml) for 24 h (*a*) or pretreated with anti-CD44 for 1 h followed by no HA treatment (*c*) or with 24 h of HA treatment (*d*)) were incubated with various concentrations of paclitaxel (3.2×10^{-9} to 1×10^{-5} M). *II, panel B, a–d,* MCF-7 cells (transfected with NanogcDNA (*a*) or treated with scrambled sequence siRNA plus 24 h of HA (50 μg/ml) treatment (*b*) or treated with NanogsiRNA plus 24 h of HA treatment (*c*) or Stat-3siRNA plus 24 h HA of treatment (*d*)) were incubated with various concentrations of paclitaxel (3.2×10^{-9} to 1×10^{-5} M). *II, panel C, a–d,* MCF-7 cells (transfected with vector alone plus 24 h HA (50 μg/ml) treatment (*a*) or no HA (*b*) or transfected with ARDcDNA with no HA (*c*) or with 24 h HA treatment (*d*)) were incubated with various concentrations of paclitaxel (3.2×10^{-9} to 1×10^{-5} M).

such as doxorubicin and paclitaxel in both breast and ovarian tumor cells. Moreover, Nanog overexpression (by transfecting MCF-7 cells and SK-OV-3.ipl cells, respectively, with NanogcDNA) drastically increases multidrug resistance in both MCF-7 cells and SK-OV-3.ipl cells (Fig. 7, *I, panel B,* and *II, panel B,* and Tables 4 and 5). Down-regulation of the expression of Nanog or Stat-3 (by transfecting tumor cells with NanogsiRNA or Stat-3siRNA) effectively enhances multidrug sensitivity in both MCF-7 cells and SK-OV-3.ipl cells (Fig. 7, *I, panel B,* and *II, panel B,* and Tables 4 and 5). These results strongly support the notion that the Nanog-Stat-3 signaling pathway is required for HA/CD44-mediated multidrug resistance in both breast and ovarian cancers.

Regulation of Drug Efflux/Retention and Multidrug Resistance in MCF-7 and SK-OV-3.ipl Cells by HA/CD44-mediated Ankyrin Function—MDR1 (P-gp) belongs to the ATP-binding cassette transporters, a superfamily of channel proteins (45–48). The functions of MDR1 (P-glycoprotein) include the efflux and retention of ions, nutrients, lipids, amino acids, peptides, proteins, and drugs (45–48). Previously, MDR1 (P-gp) was found to be associated with actin through ERM proteins in lymphoid cells (84). However, the mechanisms underlying MDR1 (P-gp) and cytoskeleton-regulated multidrug efflux in epithelial tumor cells (*e.g.* breast and ovarian tumor cells) remain unknown.

CD44 interacts with a number of membrane-associated cytoskeletal proteins, such as ankyrin, which are expressed in both breast and ovarian tumor cells (14, 19–21, 32, 43, 44). It binds directly to the ARD of ankyrin through a conserved ankyrin-binding domain in the CD44 cytoplasmic region (32). This CD44-ankyrin interaction causes cytoskeleton activation and results in several important HA-mediated functions, including channel flux activities (43). CD44 is also closely involved in MDR1 (P-glycoprotein)

TABLE 4

IC_{50} analyses of doxorubicin and paclitaxel in MCF-7 and effects of various agents on the IC_{50} of doxorubicin and paclitaxel in MCF-7 cells

Treatments	Doxorubicin (IC_{50})		Paclitaxel (IC_{50})	
	−HA	+HA	−HA	+HA
	nM		nM	
A. Effects of anti-CD44 antibody treatment on the IC_{50} values of doxorubicin and paclitaxel in HA-treated MCF-7 cells				
Untreated cells (control)	63 ± 2	316 ± 15	40 ± 2	158 ± 6
Rat anti-CD44-treated cells	52 ± 3	51 ± 2	24 ± 1	23 ± 1
B. Effects of NanogsiRNA and Stat-3siRNA treatments on the IC_{50} values of doxorubicin and paclitaxel in HA-treated MCF-7 cells				
Scrambled siRNA-treated cells	61 ± 1	314 ± 12	42 ± 2	156 ± 7
NanogsiRNA-treated cells	42 ± 1	41 ± 2	25 ± 1	23 ± 1
Stat-3siRNA-treated cells	43 ± 1	40 ± 1	25 ± 1	31 ± 1
C. Effects of Nanog and ARD overexpression on the IC_{50} values of doxorubicin and paclitaxel in HA-treated MCF-7 cells				
Vector-transfected cells	62 ± 3	315 ± 10	40 ± 2	155 ± 6
NanogcDNA-transfected cells	354 ± 14	500 ± 25	177 ± 5	199 ± 4
ARDcDNA-transfected cells	32 ± 1	31 ± 2	24 ± 1	25 ± 1

TABLE 5

Effects of various agents on the IC_{50} of doxorubicin and paclitaxel in SK-OV-3.ipl cells

Treatments	Doxorubicin (IC_{50})		Paclitaxel (IC_{50})	
	−HA	+HA	−HA	+HA
	nM		nM	
A. Effects of anti-CD44 antibody treatment on the IC_{50} of doxorubicin and paclitaxel in HA-treated SK-OV-3.ipl cells				
Untreated cells (control)	354 ± 13	1995 ± 71	158 ± 5	1000 ± 34
Rat anti-CD44-treated cells	199 ± 10	196 ± 10	125 ± 6	123 ± 5
B. Effects of NanogsiRNA and Stat-3siRNA treatments on the IC_{50} of doxorubicin and paclitaxel in HA-treated SK-OV-3.ipl cells				
Scrambled siRNA-treated cells	316 ± 13	2000 ± 82	141 ± 5	1005 ± 37
NanogsiRNA-treated cells	177 ± 8	180 ± 8	127 ± 5	128 ± 6
Stat-3siRNA-treated cells	176 ± 7	223 ± 10	126 ± 4	141 ± 7
C. Effects of Nanog and ARD overexpression on the IC_{50} of doxorubicin and paclitaxel in HA-treated SK-OV-3.ipl cells				
Vector-transfected cells	316 ± 12	1995 ± 21	140 ± 2	1005 ± 16
NanogcDNA-transfected cells	2511 ± 14	4466 ± 25	1258 ± 15	1584 ± 14
ARDcDNA-transfected cells	141 ± 1	158 ± 2	112 ± 10	125 ± 6

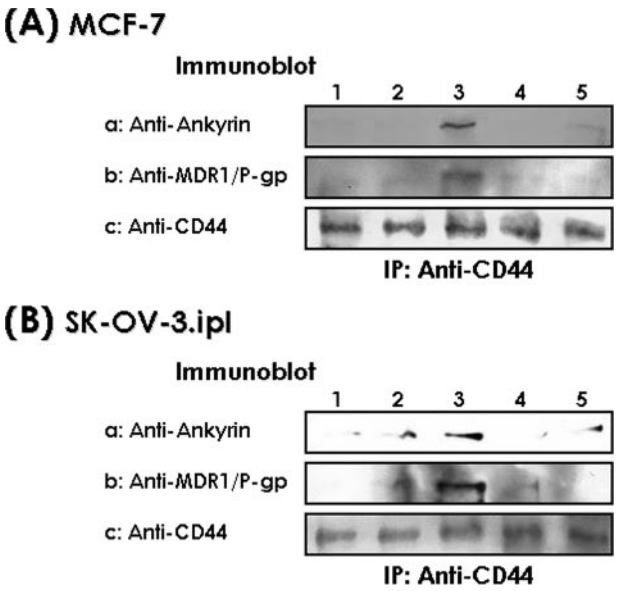

FIGURE 8. **Analysis of HA-mediated CD44 interaction with ankyrin and MDR1 (P-gp) in MCF-7 cells (*A*) and SK-OV-3.ipl cells (*B*).** Cell lysates isolated from MCF-7 cells (*A*) or SK-OV-3.ipl cells (*B*) (untreated (*lane 1*) or pretreated with anti-CD44 antibody (10 μg/ml) for 1 h followed by 5 min of HA (50 μg/ml) treatment (*lane 2*) or treated with HA (50 μg/ml) for 5 min (*lane 3*) or transfected with ARDcRNA with no HA (*lane 4*) or transfected with ARDcDNA with 5 min of HA treatment (*lane 5*)) were immunoprecipitated (*IP*) with anti-CD44 antibody followed by immunoblotting with anti-ankyrin antibody (*a*), or anti-MDR1 (P-gp) antibody (*b*), or reblotted with anti-CD44 antibody (*c*) (as a loading control).

functions in T-lymphocytes (85). The question whether the membrane-binding domain of ankyrin (*i.e.* the ARD) is involved in regulating HA/CD44-mediated MDR1 (P-gp) channel activities in epithelial tumor cells (*e.g.* breast and ovarian tumor cells) is addressed in this study.

Using anti-CD44-mediated immunoprecipitation followed by anti-ankyrin and anti-MDR1 (P-gp)-mediated immunoblotting of vector-transfected cells (treated with HA or no HA), we have found that both MDR1 (P-gp) and ankyrin are complexed with CD44 isolated from vector-transfected cells (treated with HA) (Fig. 8, *A, lane 2,* and *B, lane 2*) compared with the MDR1 (P-gp)/ankyrin-CD44 complexes isolated from vector-transfected cells treated with no HA (Fig. 8, *A, lane 1,* and *B, lane 1*) and anti-CD44 antibody plus HA (Fig. 8, *A, lane 3,* and *B, lane 3*). In contrast, neither ankyrin nor MDR1 (P-gp) becomes associated with CD44 in tumor cells transfected with a dominant-negative form of ankyrin (ARD)cDNA, either in the presence of HA (Fig. 8, *A, lane 4,* and *B, lane 4*) or in the absence of HA (Fig. 8, *A, lane 5,* and *B, lane 5*). These observations suggest that ankyrin plays an important role in HA/CD44-mediated recruitment of MDR1 (P-gp) in the plasma membrane.

In addition, we have used radioactively labeled chemotherapeutic drugs such as [^{14}C]doxorubicin and [^{3}H]paclitaxel to measure drug effluxes after HA binding to CD44-positive MCF-7 cells and SK-OV-3.ipl cells. Our results clearly show that the efflux of both doxorubicin and paclitaxel are elevated shortly after the addition of HA to vector-transfected tumor cells in a time-dependent manner reaching a plateau level ~3 h after HA addition (Fig. 9, *A–D*). Consequently, high levels of HA-mediated drug efflux cause low levels of intracellular drug retention (Table 7) and multidrug resistance (Fig. 7, *I, panels A–C,* and *II, panels A–C*; Tables 4 and 5). It is also noted that HA-mediated drug efflux activities are relatively low in vector-transfected cells without HA treatment or pretreated with anti-CD44 antibody followed by HA addition (Fig. 9, *A, a–c, B, a–c, C, a–c,* and *D, a–c*). The reduction in drug efflux activities in these cells results in an increase in intracellular drug retention (Table 7) and a reduction in multidrug resistance (Fig. 7, *I, panel C,* and *II, panel C,* and Tables 4 and 5). Moreover, we have found that overexpression of ARD by transfecting tumor cells with ARDcDNA blocks HA-mediated drug efflux leading to increase in drug retention and enhancement of multidrug sensitivities (Fig. 9, *A, d* and *f, B, d* and *f, C, d* and *e,* and *D, d* and *e*; and Table 7). In an additional control experiment, we have found that hyaluronidase (PH20)-degraded HA fails to stimulate increased drug resistance (Table 6) and efflux of chemotherapy agents

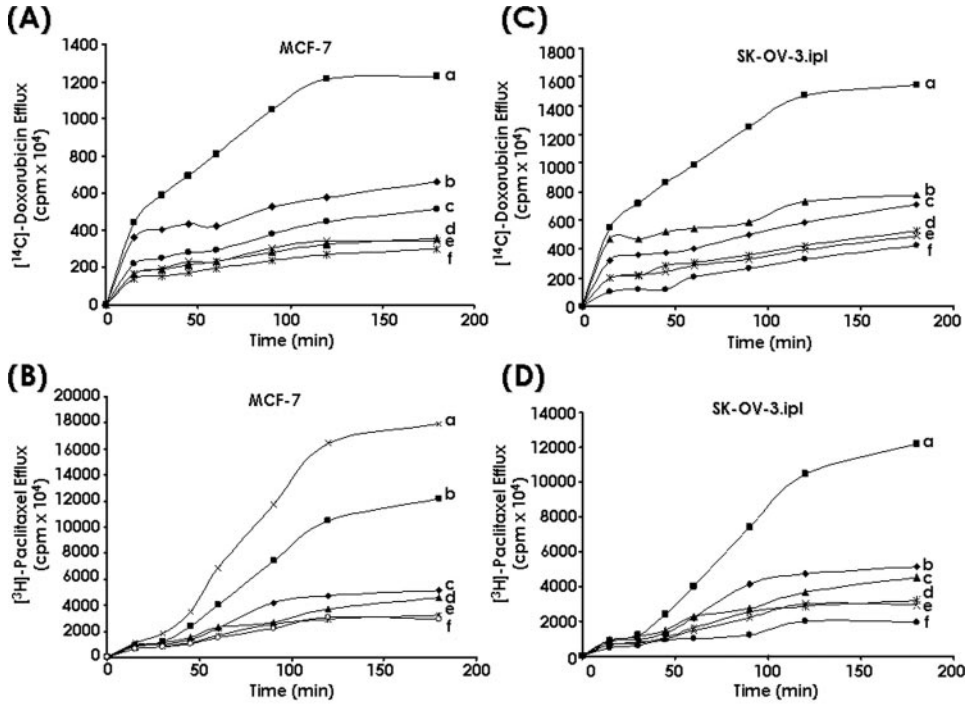

FIGURE 9. **Measurement of the drug efflux activities in MCF-7 cells (*A* and *B*) and SK-OV-3.ipl cells (*C* and *D*).** For analyzing the kinetics of drug efflux, tumor cells (transfected with ARDcDNA or vector alone) treated with either [^{14}C]doxorubicin or [^{3}H]paclitaxel for 24 h were washed and incubated with drug-free medium containing HA (50 μg/ml) or no HA or anti-CD44 antibody plus HA or PH20-treated HA. Subsequently, aliquots (100 μl) of medium were removed at various time intervals (0, 20, 40, 60, 90, 120, and 180 min). The efflux activities of [^{14}C]doxorubicin or [^{3}H]paclitaxel in MCF-7 cells (*A* and *B*) or SK-OV-3.ipl cells (*C* and *D*) were measured according to the procedures described under "Materials and Methods." *A,* efflux activities of [^{14}C]doxorubicin in MCF-7 cells (transfected with vector plus HA (*a*) or no HA (*b*), or pretreated with anti-CD44 antibody plus HA (*c*), or transfected with ARDcDNA plus HA (*d*), or PH20-treated HA (*e*), or no HA (*f*)). *B,* efflux activities of [^{3}H]paclitaxel in MCF-7 cells (transfected with vector plus HA (*a*) or no HA (*b*) or pretreated with anti-CD44 antibody plus HA (*c*), or transfected with ARDcDNA plus HA (*d*), or PH20-treated HA (*e*), or no HA (*f*)). *C,* efflux activities of [^{14}C]doxorubicin in SK-OV-3.ipl cells (transfected with vector plus HA (*a*) or no HA (*b*) or pretreated with anti-CD44 antibody plus HA (*c*), or transfected with ARDcDNA plus HA (*d*), or no HA (*e*), or PH-20-treated HA (*f*)). *D,* efflux activities of [^{3}H]paclitaxel in SK-OV-3.ipl cells (transfected with vector plus HA (*a*) or no HA (*b*) or pretreated with anti-CD44 antibody plus HA (*c*), or transfected with ARDcDNA plus HA (*d*), or no HA (*e*), or PH20-treated HA (*f*)).

TABLE 6

Effects of PH-20-treated HA on the IC_{50} of doxorubicin and paclitaxel in SK-OV-3.ipl cells

IC_{50} is designated as "the nM concentration of chemotherapeutic drugs (*e.g.* doxorubicin or paclitaxel) that causes 50% inhibition of tumor cell growth." IC_{50} values are presented as the means ± S.D. All assays consisted of at least six replicates and were performed on at least three different experiments.

Cells	Doxorubicin (IC_{50})		Paclitaxel (IC_{50})	
	−HA	+PH20-treated HA	−HA	+PH20-treated HA
	nM		nM	
MCF-7 cells	60 ± 3	51 ± 2	38 ± 2	30 ± 2
SK-OV-3.ipl cells	310 ± 6	275 ± 5	138 ± 3	104 ± 4

(Fig. 9, *A, e, B, e, C, f,* and *D, f*) in tumor cells. Therefore, we conclude that multidrug efflux/retention and resistance is HA/CD44-specific and ankyrin-dependent in both breast and ovarian tumor cells. Interference of the endogenous ankyrin binding to CD44 (using overexpression of ARD fragments by transfecting cells with ARDcDNA) not only abolishes MDR1 (P-gp) association with ankyrin in CD44-containing plasma membrane (Fig. 8) but also significantly modulates multidrug efflux/retention (Fig. 9) and decreases HA/CD44-mediated multidrug resistance (Fig. 7, *I, panel C,* and *II, panel C*; Tables 4 and 5). These results clearly indicate that the CD44-ankyrin interaction plays an important role in regulating MDR1 (P-gp)-linked drug efflux/retention and multidrug resistance.

DISCUSSION

Multidrug resistance is a challenging clinical problem in the treatment of both breast and ovarian cancers (1). The most commonly used anti-tumor agents in the treatment of disseminated breast or ovarian cancers include doxorubicin and paclitaxel (Taxol) (86, 87). The ability of doxorubicin to bind DNA and/or produce free radicals is thought to be possible mechanisms to induce cytotoxic effects on tumor cells (88). Paclitaxel is known to bind a subunit of the tubulin heterodimers that form cellular microtubules (89). The paclitaxel-cytoskeleton interaction accelerates tubulin polymerization and inhibits the depolymerization of microtubules resulting in an inactivation of the mitotic checkpoint and tumor cell killing (90). Resistance to chemotherapeutic drugs used in breast and ovarian cancer treatments (*e.g.* doxorubicin and paclitaxel) is often associated with overexpression of the multidrug resistance gene 1 (MDR1 or P-glycoprotein (P-gp)) (91). The MDR1 gene product functions as a drug efflux pump actively reducing intracellular drug concentrations in resistant tumor cells (45–48). However, the biological factors determining the ability of certain breast and ovarian epithelial cells to overexpress the *MDR1* gene and display the multidrug-resistant phenotype remain unknown. It is currently very difficult to predict the efficacy of any particular chemotherapeutic drug treatment. Thus, there is a great need to clarify the tumor biology mechanisms underlying the clinical behavior of multidrug resistance in both breast and ovarian tumor cells.

A number of studies have aimed at identifying molecules expressed by epithelial tumor cells (*e.g.* breast and ovarian tumor cells) that correlate with metastatic behavior and chemoresistance. Among such candidates are HA, a major component in the ECM of most mammalian tissues (5, 6), and CD44, a major HA receptor (31). Both HA and CD44 are overexpressed at sites of tumor attachment (9, 10, 13–28) and appear to be closely involved in multidrug resistance during solid tumor progression (52–55). A previous study using breast tumor cells found that *MDR1* expression and multidrug resistance are

TABLE 7

Measurement of drug retention in both MCF-7 and SK-OV-3.ipl cells

For analyzing drug retention, tumor cells (transfected with ARDcDNA or vector alone) treated with either [^{14}C]doxorubicin or [^{3}H]paclitaxel for 24 h were washed and incubated in drug-free medium containing HA (50 μg/ml) or no HA or anti-CD44 antibody plus HA for 2 h. After the medium was aspirated, cells were washed twice and then harvested. Cell numbers were measured by a hemocytometer and then dissolved in Solvable tissue gel solubilizer. Radioactivity associated with cells (indicated as intracellular drug retention) was then measured by liquid scintillation counter as described under "Materials and Methods." The retention level of [^{14}C]doxorubicin or [^{3}H]paclitaxel in MCF-7 cells or SK-OV-3.ipl cells (transfected with ARDcDNA (or vector alone) in the presence or absence of HA (or pretreated with anti-CD44 plus HA)) were conducted according to the procedures described under "Materials and Methods." Tumor cells transfected with vector alone in the absence of HA is designated as 100% (control). For the drug retention assay, data represent mean ± S.E. of the amount of radioactively labeled drug-associated with cells in each sample.

Treatments	MCF-7 cells		SK-OV-3.ipl cells	
	[^{14}C]Doxorubic in cpm	[^{3}H]Paclitaxel in cpm	[^{14}C]Doxorubic in cpm	[^{3}H]Paclitaxel cpm
	% control[a]	*% control*[b]	*% control*[c]	*% control*[d]
Vector-transfected cells treated with no HA (control)	100 ± 2	100 ± 4	100 ± 2	100 ± 6
Vector-transfected cells treated with HA	51 ± 1[a]	48 ± 2[b]	39 ± 1[c]	32 ± 1[d]
Vector-transfected cells pretreated with anti-CD44 plus HA	205 ± 8[a]	248 ± 9[b]	143 ± 2[c]	158 ± 6[d]
ARDcDNA-transfected cells treated with no HA	201 ± 4[a]	220 ± 8[b]	157 ± 4[c]	163 ± 6[d]
ARDcDNA-transfected cells treated with HA	202 ± 5[a]	212 ± 5[b]	168 ± 5[c]	185 ± 7[d]

[a] Data are significantly different ($p < 0.001$; ANOVA; $n = 5$) as compared with control samples (*e.g.* vector-transfected (control) treated with no HA samples).
[b] Data are significantly different ($p < 0.005$; ANOVA; $n = 6$) as compared with control samples (*e.g.* vector-transfected (control) treated with no HA samples).
[c] Data are significantly different ($p < 0.005$; ANOVA; $n = 5$) as compared with control samples (*e.g.* vector-transfected (control) treated with no HA samples).
[d] Data are significantly different ($p < 0.001$; ANOVA; $n = 5$) as compared with control samples (*e.g.* vector-transfected (control) treated with no HA samples).

linked to a positive feedback circuit involving HA, phosphoinositide 3-kinase, and ErbB2 (52). The results of a recent study on lymphoma cells indicate that HA can modulate the drug sensitivity by regulating MDR-1 (P-gp) pump activity and phosphoinositide 3-kinase/AKT pathways (85). In addition, HA-CD44-induced Ca^{2+} signaling (53) and epidermal growth factor receptor activation (54) have been shown to play an important role in drug resistance. HA-CD44 interaction also influences topoisomerase II activity and etoposide cytotoxicity in head and neck cancers (55). These findings suggest that HA-CD44 interaction is definitely involved in multidrug resistance. The following questions are addressed in this study. (i) Which HA/CD44-mediated signaling pathway controls *MDR-1* gene expression? (ii) How is HA/CD44-mediated drug efflux/retention by MDR-1 (P-gp)s regulated in epithelial tumor cells (*e.g.* breast and ovarian tumor cells)?

Cancer stem cells found in solid tumors (including breast and ovarian cancers) have been implicated in both the initiation/development of malignancy and multidrug resistance (60, 61). Tumor cells derived from cancer stem cells display heterogeneous phenotypes of the parental cancer cells. For example, some cancer stem cells have lost their ability to control normal stem cell numbers, pluripotence, and lineage differentiation (62–65). These findings suggest that tumor formation may be related to an alteration of stem cell function. Both Nanog (a transcription factor initially detected in embryonic stem cells) and CD44 are considered to be important molecules in cancer stem cell functions occurring during both breast and ovarian cancer progression (13–28, 68, 69), but their interaction with each other during tumor progression has not been investigated. In this study we have identified the presence of Nanog in both breast and ovarian tumor cells (Fig. 1). To further characterize the role of Nanog in these tumor cells, we have found a close, physical interaction between Nanog and CD44 in both MCF-7 cells and SK-OV-3.ipl cells (Fig. 2). Most importantly, the binding of HA to CD44 promotes Nanog association with CD44, nuclear translocation, and subsequent target gene expression (*e.g.* pluripotent stem cell regulators, Rex1 and Sox2) (Fig. 3). Therefore, it is likely that the HA-CD44 interaction serves as an upstream activator of Nanog signaling. Because aberrant expression of pluripotency-associated genes has been shown to be closely associated with aggressive cancer progression (68, 69), it is possible that under the influence of an abnormal HA-enriched ECM environment, CD44-expressing tumor cells are reprogrammed to acquire certain stem cell marker-related properties, including self-renewal and tumor cell growth/survival required for chemotherapy resistance.

A recent study shows that among 11 pseudogenes derived from the *Nanog* gene, NANOGP8 appears to be unique based on its sequence homology with Nanog and its retrogene-like (not pseudogene) properties (92). In fact, NANOGP8 expression is detected in a number of tumor cells, and it has also been closely associated with cell proliferation (92). The question of whether NANOGP8 plays a role in epithelial tumor progression is currently under investigation in our laboratory.

Stat-3, a member of the Janus-activated kinase/Stat signaling pathway (70, 71), plays an important role in regulating a variety of biological activities in both normal and tumor cells (70–73). Stat-3 signaling can be activated by cytokines and growth factors as well as oncogenic proteins (*e.g.* Src and Ras) (93, 94). For example, tyrosine phosphorylation of Stat-3 by Src induces Stat-3 dimerization followed by interaction with specific promoter elements of target genes that regulate the expression of proliferation and anti-apoptotic proteins (70–73, 75, 76). In this study we have observed that Nanog binds to Stat-3 in both breast and ovarian tumor cells during HA/CD44-mediated signaling (Fig. 4). Specifically, HA treatment of MCF-7 cells and SK-OV-3.ipl cells causes a significant increase in the amount of Stat-3 bound to Nanog (in the nucleus) and stimulates Stat-3-specific transcriptional activation (Fig. 5) leading to *MDR1* (*P-gp*) gene expression (Fig. 6) and tumor cell growth (Tables 1–3), as well as multidrug resistance (Fig. 7 and Tables 4 and 5). Further analyses show that Nanog overexpression (by transfecting cells with NanogcDNA) effectively stimulates endogenous Nanog association with Stat-3, Stat-3-specific transcriptional activation, *MDR1* (*P-gp*) gene expression (Fig. 6), and chemoresistance (Tables 4 and 5). These findings clearly indicate that stem cell marker, Nanog (mimicking HA stimulation), is an activator of oncogenic signaling and *MDR1*(*P-gp*) gene expression.

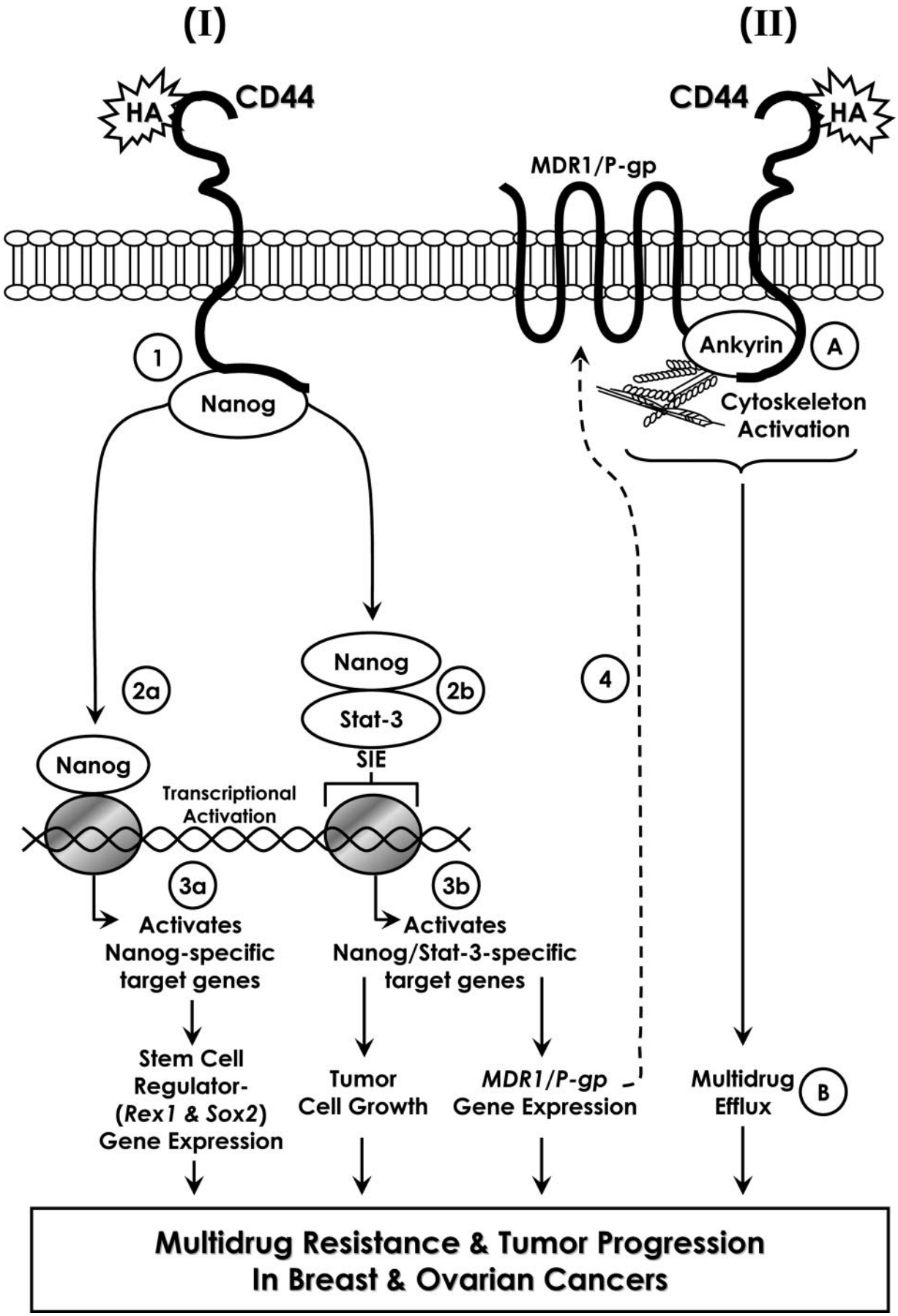
(I)
(II)
HA
CD44
CD44
HA
MDR1/P-gp
Ankyrin
A
1
Nanog
Cytoskeleton
Activation
Nanog
2b
Stat-3
SIE
4
2a
Nanog
Transcriptional
Activation
3a
3b
Activates
Nanog-specific
target genes
Activates
Nanog/Stat-3-specific
target genes
Stem Cell
Regulator-
(*Rex1* & *Sox2*)
Gene Expression
Tumor
Cell Growth
MDR1/P-gp
Gene Expression
Multidrug
Efflux
B
Multidrug Resistance & Tumor Progression
In Breast & Ovarian Cancers

Moreover, we have observed that HA/CD44-mediated Stat-3 signaling and transcriptional activation are significantly inhibited when both Nanog and Stat-3 are down-regulated (by treating cells with NanogsiRNA or Stat-3siRNA). Most importantly, these treatments result in an increased chemosensitivity of MCF-7 cells and SK-OV-3.ipl cells to doxorubicin and paclitaxel (Fig. 7 and Tables 4 and 5). Thus, these results provide strong evidence that both Nanog and Stat-3 act as novel signaling molecules that connect HA-CD44 signaling to the activation of newly identified Stat-3-specific target genes (encoding MDR1 (P-gp) involved in chemoresistance) in both breast and ovarian tumor cells. These observations are consistent with previous reports that cancer stem cells displaying MDR1 overexpression and Stat-3 up-regulation are likely to be responsible both for disease relapse and the resistance to therapy that often accompanies relapse (95–97).

The binding of HA to CD44 also triggers direct cross-talk between several different tyrosine kinase (*e.g.* $p185^{HER2}$ tyrosine kinase and c-Src kinase)-linked signaling pathways (19–21). In addition, certain angiogenic factors (*e.g.* vascular endothelial growth factor or basic fibroblast growth factor) and matrix-degradation enzymes also become tightly complexed with CD44 suggesting that they play a synergistic role in the generation of oncogenic signals leading to tumor-specific behaviors (19–21) and multidrug resistance (52–55). Most importantly, during HA signaling the cytoplasmic domain of CD44 appears to select a unique downstream effector (specifically, the cytoskeletal protein ankyrin) that links ECM and the cytoskeleton in tumor cells (19–21). Ankyrin contains three functional domains as follows: a conserved N-terminal ARD consisting of 22–24 tandem repeats of 33 amino acids; a spectrin/fodrin-binding domain; and a variably sized C-terminal regulatory domain (33, 41, 42). CD44 binds directly to the ARD of ankyrin through a conserved ankyrin-binding domain in the CD44 cytoplasmic region (32). This CD44-ankyrin interaction induces cytoskeleton activation and results in several important HA-mediated functions (14, 19–21, 32, 43, 44). A previous study showed that CD44-P-gp interaction promotes cell migration and invasion in cancer (56). In addition, ankyrin is known to play an important role in tumor cell migration and invasion in tumor cells (14, 19–21, 32, 43, 44). The fact that ankyrin is closely linked to CD44 and MDR1 (P-gp) in tumor cells suggests that an ankyrin-based cytoskeleton plays an important role in cell migration/invasion in these tumor cells.

Previous studies showed that MDR1 (P-gp) co-localized with CD44 and the cytoskeleton in a complex (98) that may be related to the still poorly understood regulation of MDR1 (P-gp)-mediated multidrug transport functions. In addition, we have found that HA-CD44 interaction stimulates recruitment of the cytoskeletal protein, ankyrin, and inositol 1,4,5-triphosphate receptor (an inositol 1,4,5-triphosphate-gated calcium channel) into plasma membrane leading to intracellular calcium (Ca^{2+}) mobilization and several important cellular functions such as cell adhesion, secretion, and proliferation (43). Ankyrin also binds to intracellular Ca^{2+} channels such as the ryanodine receptor and modulates Ca^{2+} fluxes (99). Ankyrin repeat-like polypeptides are also implicated in the regulation of a number of plasma membrane-associated ion and drug pumps (100, 101).

In this study we have presented new evidence indicating that ankyrin interacts with both CD44 and MDR1 (P-gp) (Fig. 8). Specifically, we have demonstrated that HA treatment promotes ankyrin linkage to CD44 and MDR-1 (P-gp) to form a multiple molecular complex *in vivo* (Fig. 8). Functional studies indicate that ankyrin binding to CD44 and MDR-1 (P-gp) is involved in HA-mediated multidrug efflux (Fig. 9) and retention (Table 7). Furthermore, we have found that the failure to recruit ankyrin and MDR1 (P-gp) into a complex with CD44 using overexpression of ARD fragments (by transfecting cells with ARDcDNA) abolishes active multidrug efflux (Fig. 9), increases drug retention (Table 7), reduces HA/CD44-mediated multidrug resistance, and enhances chemosensitivity (Tables 4 and 5). Thus ARD fragment of ankyrin acts as a potent competitive inhibitor capable of interfering with the endogenous ankyrin interaction between CD44 and MDR1 (P-gp) during HA-mediated multidrug fluxes and chemoresistance. Taken together, our results strongly support the conclusion that the HA/CD44-mediated Nanog-Stat-3 signaling pathway and ankyrin-cytoskeleton interaction may serve as new cellular targets for sensitizing chemotherapy drug treatments for both breast and ovarian tumor cells displaying stem cell-like properties. Furthermore, in Table 7 we have shown that anti-CD44 antibody not only blocks HA binding but also inhibits MDR-1-mediated efflux activity leading to an increase in drug retention. Thus, in the future, anti-CD44 antibody may be used in combination with various chemotherapeutic drugs for enhancing chemosensitivity during the treatment of breast and/or ovarian cancers.

As summarized in Fig. 10, we would like to propose that upon binding of HA, CD44 is first tightly coupled with Nanog in a complex (*I, step 1*) followed by an increase of Nanog in the nucleus. Nanog then causes transcriptional activation (Fig. 10*I, step 2a*) and the expression of its target genes such as *Rex1* and *Sox2* (*I, step 3a*). Some Nanog also forms a complex with Stat-3 in the nucleus (Fig. 10*I, step 2b*) and induces Stat-3-specific transcriptional activation (*I, step 3b*) leading to tumor cell growth and *MDR-1* gene expression (and localization at the plasma membrane) (*I, step 4*). Furthermore, HA binding promotes ankyrin-MDR1 (P-gp) association with CD44 (Fig. 10*II, step A*). This complex formation results in an efflux of chemo-

FIGURE 10. **A proposed model for CD44 interaction with Nanog signaling (*I*) and ankyrin (*II*) during HA-activated multidrug resistance and tumor progression.** *I,* upon binding of HA, CD44 is first tightly coupled with Nanog in a complex (*step 1*) followed by an increase of Nanog in the nucleus. Nanog then causes transcriptional activation (*step 2a*) and the expression of its target genes such as *Rex1* and *Sox2* (*step 3a*). Some Nanog also forms a complex with Stat-3 in the nucleus and induces Stat-3-specific transcriptional activation (*step 2b*) leading to tumor cell growth and *MDR-1* gene expression (*step 3b*) (and localization at the plasma membrane) (*step 4*); *II,* HA binding also promotes ankyrin-MDR1 (P-gp) association with CD44 (*step A*). This complex formation results in an efflux of chemotherapeutic drugs (*step B*). The coordinated HA-mediated CD44 activation of Nanog/Nanog-Stat-3 signaling (*I*) and the ankyrin-based cytoskeleton (*II*) is proposed as a possible mechanism underlying various tumor stem cell-specific behaviors, including transcriptional activation, tumor cell growth, and multidrug resistance during both breast and ovarian tumor progression.

therapeutic drugs (Fig. 10*II, step B*). The coordinated HA-mediated CD44 activation of Nanog/Nanog-Stat-3 signaling (*I*) and the ankyrin-based cytoskeleton (*II*) (as diagrammed in Fig. 10) is proposed as a possible mechanism underlying various tumor stem cell-specific behaviors, including transcriptional activation, tumor cell growth, and multidrug resistance during both breast and ovarian tumor progression.

Acknowledgments—We gratefully acknowledge assistance from Dr. Gerard J. Bourguignon in the preparation of this paper. We are also grateful to Christina Camacho for help in preparing graphs and illustrations.

REFERENCES

1. Harnett, P. R., Kirsten, F., and Tattersall, M. H. (1986) *J. Clin. Oncol.* **4,** 952–957
2. Mollinedo, F. (2005) *IDrugs* **8,** 127–143
3. Hehlgans, S., Haase, M., and Cordes, N. (2007) *Biochim. Biophys. Acta* **1775,** 163–180
4. Nishio, K., and Saijo, N. (1999) *Anticancer Drug Des.* **14,** 133–141
5. Laurent, T. C., and Fraser, J. R. E. (1992) *FASEB J.* **6,** 2397–2404
6. Lee, J. Y., and Spicer, A. P. (2000) *Curr. Opin. Cell Biol.* **12,** 581–586
7. Toole, B. P. (2001) *Semin. Cell Dev. Biol.* **12,** 79–87
8. Stern, R., and Jedrzejas, M. J. (2006) *Chem. Rev.* **106,** 818–839
9. Knudson, W., Biswa, C., Li, X., Nemec, R. E., and Toole, B. P. (1989) *CIBA Found. Symp.* **143,** 150–159
10. Toole, B. P., Wight, T., and Tammi, M. (2002) *J. Biol. Chem.* **277,** 4593–4596
11. Delpech, B., Cheyallier, B., Reinhardt, N., Julien, J. P., Duval, C., Maingonnat, C., Bastit, P., and Asselain, B. (1990) *Int. J. Cancer* **46,** 388–390
12. Jones, L. M. H., Gardner, J. B., Catterall, J. B., and Turner, G. A. (1995) *Clin. Exp. Metastasis* **13,** 373–380
13. Iida, N., and Bourguignon, L. Y. W. (1995) *J. Cell Physiol.* **162,** 127–133
14. Zhu, D., and Bourguignon, L. Y. W. (1998) *Cell Motil. Cytoskeleton* **39,** 209–222
15. Iida, N., and Bourguignon, L. Y. W. (1997) *J. Cell Physiol.* **171,** 152–160
16. Bourguignon, L. Y. W., Zhu, H. B., Chu, A., Zhang, L., and Hung, M. C. (1997) *J. Biol. Chem.* **272,** 27913–27918
17. Gunthert, U., Hoffman, M., Rudy, W., Reber, S., Zoller, M., Haussmann, I., Matzku, S., Wenzel, A., Ponta, H., and Herrlich, P. (1991) *Cell* **65,** 13–24
18. Auvinen, P., Tammi, R., Tammi, M., Johansson, R., and Kosma, V. M. (2005) *Histopathology* **47,** 420–428
19. Bourguignon, L. Y. W. (2001) *J. Mammary Gland Biol. Neoplasia* **6,** 287–297
20. Bourguignon, L. Y. W., Zhu, D., and Zhu, H. (1998) *Front. Biosci.* **3,** 637–649
21. Turley, E. A., Nobel, P. W., and Bourguignon, L. Y. W. (2002) *J. Biol. Chem.* **277,** 4589–4592
22. Bourguignon, L. Y. W., Gunja-Smith, Z., Iida, N., Zhu, H. B., Young, L. J. T., Muller, W., and Cardiff, R. D. (1998) *J. Cell Physiol.* **176,** 206–215
23. Bourguignon, L. Y. W., Zhu, H., Shao, L., Zhu, D., and Chen, Y. W. (1999) *Cell Motil. Cytoskeleton* **43,** 269–287
24. Bourguignon, L. Y. W., Singleton, P., Zhu, H., and Diedrich, F. (2003) *J. Biol. Chem.* **278,** 29420–29434
25. Bourguignon, L. Y. W., Zhu, H., Shao, L., and Chen, Y. W. (2000) *J. Biol. Chem.* **275,** 1829–1838
26. Bourguignon, L. Y. W., Zhu, H., Zhou, B., Diedrich, F., Singleton, P. A., and Hung, M. C. (2001) *J. Biol. Chem.* **276,** 48679–48692
27. Bourguignon, L. Y. W., Zhu, H., Shao, L., and Chen, Y. W. (2001) *J. Biol. Chem.* **276,** 7327–7336
28. Bourguignon, L. Y. W., Singleton, P., Zhu, H., and Zhou, B. (2002) *J. Biol. Chem.* **277,** 39703–39712
29. Screaton, G. R., Bell, M. V., Jackson, D. G., Cornelis, F. B., Gerth, U., and Bell, J. I. (1992) *Proc. Natl. Acad. Sci. U. S. A.* **89,** 12160–12164
30. Screaton, G. R., Bell, M. V., Bell, J. I., and Jackson, D. G. (1993) *J. Biol. Chem.* **268,** 12235–12238
31. Underhill, C. (1992) *J. Cell Sci.* **103,** 293–298
32. Zhu, D., and Bourguignon, L. Y. W. (2000) *J. Cell. Physiol.* **183,** 182–195
33. Bennett, V., and Baines, A. J. (2001) *Physiol. Rev.* **81,** 1353–1392
34. Lambert, S., Yu, H., Prchal, J. T., Lawler, J., Ruff, P., Speicher, D., and Palek, J. (1990) *Proc. Natl. Acad. Sci. U. S. A.* **87,** 1730–1734
35. Lux, S. E., John, K. M., and Bennett, V. (1990) *Nature* **344,** 36–43
36. Tse, W. T., Menninger, J. C., Yang-Feng, T. L., Francke, U., Sahr, K. E., and Forget, B. G. (1991) *Genomics* **12,** 702–704
37. Otto, E., Kunimoto, M., McLaughlin, T., and Bennett, V. (1991) *J. Cell Biol.* **114,** 241–253
38. Kordeli, E., and Bennett, V. (1991) *J. Cell Biol.* **114,** 1243–1259
39. Peters, L. L., John, K. M., Lu, F. M., Eicher, E. M., and Lux, S. E. (1995) *J. Cell Biol.* **130,** 313–330
40. Peters, L. L., and Lux, S. E. (1993) *Hematology* **30,** 85–118
41. Davis, L. H., Davis, J. Q., and Bennett, V. (1992) *J. Biol. Chem.* **267,** 18966–18972
42. Davis, L., and Bennett, V. (1990) *J. Biol. Chem.* **265,** 10589–10596
43. Singleton, P. A., and Bourguignon, L. Y. W. (2004) *Exp. Cell Res.* **295,** 102–118
44. Bourguignon, L. Y. W., and Singleton, P. (2005) in *Hyaluronan–Its Structure, Metabolism, Biological Activities and Therapeutic Applications* (Balazs, E. A., and Hascall, V. C., eds) pp. 305–316, Matrix Biology Institute Press, Edgewater, NJ
45. Juliano, R. L., and Ling, V. A. (1976) *Biochim. Biophys. Acta* **455,** 152–162
46. Gros, P., Croop, J., and Housman, D. (1986) *Cell* **47,** 371–380
47. Higgins, C. F. (1992) *Annu. Rev. Cell Biol.* **8,** 67–113
48. Fojo, A. T., Ueda, K., Slamon, D. J., Poplack, D. G., Gottesman, M. M., and Pastan, I. (1987) *Proc. Natl. Acad. Sci. U. S. A.* **84,** 265–269
49. Cordo Russo, R. I., Garcia, M. G., Alaniz, L., Blanco, G., Alvarez, E., and Hajos, S. E. (2008) *Int. J. Cancer* **122,** 1012–1018
50. Ohashi, R., Takahashi, F., Cui, R., Yoshioka, M., Gu, T., Sasaki, S., Tominaga, S., Nishio, K., Tanabe, K. K., and Takahashi, K. (2007) *Cancer Lett.* **252,** 225–234
51. Misra, S., Ghatak, S., Zoltan-Jones, A., and Toole, B. P. (2003) *J. Biol. Chem.* **278,** 25285–25288
52. Misra, S., Ghatak, S., and Toole, B. P. J. (2005) *J. Biol. Chem.* **280,** 20310–20315
53. Wang, S. J., and Bourguignon, L. Y. (2006) *Arch. Otolaryngol. Head Neck Surg.* **132,** 19–24
54. Wang, S. J., and Bourguignon, L. Y. (2006) *Arch. Otolaryngol. Head Neck Surg.* **132,** 771–778
55. Wang, S. J., Peyrollier, K., and Bourguignon, L. Y. (2007) *Arch. Otolaryngol. Head Neck Surg.* **133,** 281–288
56. Miletti-González, K. E., Chen, S., Muthukumaran, N., Saglimbeni, G. N., Wu, X., Yang, J., Apolito, K., Shih, W. J., Hait, W. N., and Rodríguez-Rodríguez, L. (2005) *Cancer Res.* **65,** 6660–6667
57. Haylock, D. N., and Nilsson, S. K. (2006) *Regen. Med.* **1,** 437–445
58. Al-Hajj, M., Wicha, M. S., Benito-Hernandez, A., Morrison, S. J., and Clarke, M. F. (2003) *Proc. Natl. Acad. Sci. U. S. A.* **100,** 3983–3988
59. Sales, K. M., Winslet, M. C., and Seifalian, A. M. (2007) *Stem Cell Rev.* **3,** 249–255
60. Huang, E. H., Heidt, D. G., Li, C. W., and Simeone, D. M. (2007) *Surgery* **141,** 415–419
61. Chumsri, S., Phatak, P., Edelman, M. J., Khakpour, N., Hamburger, A. W., and Burger, A. M. (2007) *Cancer Genomics Proteomics* **4,** 165–174
62. Chambers, I., Colby, D., Robertson, M., Nichols, J., Lee, S., Tweedie, S., and Smith, A. (2003) *Cell* **113,** 643–655
63. Mitsui, K., Tokuzawa, Y., Itoh, H., Segawa, K., Murakami, M., Takahashi, K., Maruyama, M., Maeda, M., and Yamanaka, S. (2003) *Cell* **113,** 631–642
64. Kuroda, T., Tada, M., Kubota, H., Kimura, H., Hatano, S. Y., Suemori, H., Nakatsuji, N., and Tada, T. (2005) *Mol. Cell. Biol.* **25,** 2475–2485
65. Rodda, D. J., Chew, J. L., Lim, L. H., Loh, Y. H., Wang, B., Ng, H. H., and Robson, P. (2005) *J. Biol. Chem.* **280,** 24731–24737
66. Do, J. T., and Scholer, H. R. (2006) *Ernst Schering Res. Found. Workshop* **60,** 35–45

67. Lin, T., Chao, C., Saito, S., Mazur, S. J., Murphy, M. E., Appella, E., and Xu, Y. (2005) *Nat. Cell Biol.* **7,** 165–171
68. Hoei-Hansen, C. E., Kraggerud, S. M., Abeler, V. M., Kaern, J., Rajpert-De Meyts, E., and Lothe, R. A. (2007) *Mol. Cancer* **6,** 1–12
69. Ezeh, U. I., Turek, P. J., Reijo, R. A., and Clark, A. T. (2005) *Cancer* **104,** 2255–2265
70. Levy, D. E., and Lee, C. K. (2002) *J. Clin. Investig.* **109,** 1143–1148
71. Huang, S. (2007) *Clin. Cancer Res.* **13,** 1362–1366
72. Darnell, J. E., Jr. (1997) *Science* **277,** 1630–1635
73. Schindler, C., and Darnell, J. E., Jr. (1995) *Annu. Rev. Biochem.* **64,** 621–651
74. Sato, N., Meijer, L., Skaltsounis, L., Greengard, P., and Brivanlou, A. H. (2004) *Nat. Med.* **10,** 55–63
75. Vultur, A., Cao, J., Arulanandam, R., Turkson, J., Jove, R., Greer, P., Craig, A., Elliott, B., and Raptis, L. (2004) *Oncogene* **23,** 2600–2616
76. Kim, D. J., Chan, K. S., Sano, S., and DiGiovanni, J. (2007) *Mol. Carcinog.* **46,** 725–731
77. Huang, M., Page, C., Reynolds, R. K., and Lin, J. (2000) *Gynecol. Oncol.* **79,** 67–73
78. Sartor, C. I., Dziubinski, M. L., Yu, C. L., Jove, R., and Ethier, S. P. (1997) *Cancer Res.* **57,** 978–987
79. Bourguignon, L. Y, Gilad, E., and Peyrollier, K. (2007) *J. Biol. Chem.* **282,** 19426–19441
80. Bourguignon, L. Y., Peyrollier, K., Gilad, E., and Brightman, A. (2007) *J. Biol. Chem.* **282,** 1265–1280
81. Bourguignon, L. Y., Gilad, E., Rothman, K., and Peyrollier, K. (2005) *J. Biol. Chem.* **280,** 11961–11972
82. Kuh, H. J., Jang, S. H., Wientjes, M. G., and Au, J. L. (2000) *J. Pharmacol. Exp. Ther.* **293,** 761–770
83. Lassmann, S., Schuster, I., Walch, A., Göbel, H., Jütting, U., Makowiec, F., Hopt, U., and Werner, M. (2007) *J. Clin. Pathol.* **60,** 173–179
84. Luciani, F., Molinari, A., Lozupone, F., Calcabrini, A., Lugini, L., Stringaro, A., Puddu, P., Arancia, G., Cianfriglia, M., and Fais, S. (2002) *Blood* **99,** 641–648
85. Honig, S. M., Fu, S., Mao, X., Yopp, A., Gunn, M. D., Randolph, G. J., and Bromberg, J. S. (2003) *J. Clin. Investig.* **111,** 627–637
86. Muggia, F. M. (1997) *Drugs* **54,** Suppl. 4, 22–29
87. Wiseman, L. R., and Spencer, C. M. (1998) *Drugs Aging* **12,** 305–334
88. Gewirtz, D. A. (1999) *Biochem. Pharmacol.* **57,** 727–741
89. Bhalla, K. N. (2003) *Oncogene* **22,** 9075–9086
90. Wang, T. H., Wang, H. S., and Soong, Y. K. (2000) *Cancer* **88,** 2619–2628
91. Baker, E. K., and El-Osta, A. (2004) *Cancer Biol. Ther.* **3,** 819–824
92. Zhang, J., Wang, X., Li, M., Han, J., Chen, B., Wang, B., and Dai, J. (2006) *FEBS J.* **273,** 1723–1730
93. Turkson, J., Bowman, T., Garcia, R., Caldenhoven, E., De Groot, R. P., and Jove, R. (1998) *Mol. Cell. Biol.* **18,** 2545–2552
94. Turkson, J., Bowman, T., Adnane, J., Zhang, Y., Djeu, J. Y., Sekharam, M., Frank, D. A., Holzman, L. B., Wu, J., Sebti, S., and Jove, R. (1999) *Mol. Cell. Biol.* **19,** 7519–7528
95. Manara, M. C., Serra, M., Benini, S., Picci, P., and Scotlandi, K. (2004) *Int. J. Oncol.* **24,** 365–372
96. Mechetner, E., Kyshtoobayeva, A., Zonis, S., Kim, H., Stroup, R., Garcia, R., Parker, R. J., and Fruehauf, J. P. (1998) *Clin. Cancer Res.* **4,** 389–398
97. Burger, H., Foekens, J. A., Look, M. P., Meijer-van Gelder, M. E., Klijn, J. G., Wiemer, E. A., Stoter, G., and Nooter, K. (2003) *Clin. Cancer Res.* **9,** 827–836
98. Bacso, Z., Nagy, H., Goda, K., Bene, L., Fenyvesi, F., Matkó, J., and Szabó, G. (2004) *Cytometry* **61,** 105–116
99. Bourguignon, L. Y., Chu, A., Jin, H., and Brandt, N. R. (1995) *J. Biol. Chem.* **270,** 17917–17922
100. Amstutz, P., Binz, H. K., Parizek, P., Stumpp, M. T., Kohl, A., Grütter, M. G., Forrer, P., and Plückthun, A. (2005) *J. Biol. Chem.* **280,** 24715–24722
101. Singh, V. K., Zhou, Y., Marsh, J. A., Uversky, V. N., Forman-Kay, J. D., Liu, J., and Jia, Z. (2007) *Cancer Res.* **67,** 626–633
102. Lokeshwar, V. B., Iida, N., and Bourguignon, L. Y. (1996) *J. Biol. Chem.* **271,** 23853–23864
103. West, D. C., and Kumar, S. (1989) *Exp. Cell Res.* **183,** 179–196